Comparison of selected mathematical functions for the analysis of growth behavior of items and physical interpretation of Avrami−Weibull function

Porównanie wybranych funkcji matematycznych do analizy przebiegu wzrostu podmiotów oraz interpretacja funkcji Avrami'ego−Weibulla

Keshra Sangwal*

Department of Applied Physics, Lublin University of Technology, Nadbystrzycka 38, 20-618 Lublin, Poland

Abstract

Empirical data of sigmoidal-shaped $y(t)$ growth behavior of different types of items, such as papers and citations earned by individual and all successively published papers of selected top-cited authors, germination of tomato seeds and three different bacteria, are analyzed and compared by Avrami−Weibull, Verhulst (logistic) and Gompertz functions. It was found that: (1) Avrami−Weibull function describes different types of the data better than Gompertz and Verhulst funtions, and (2), in comparison with Verhulst and Gompertz functions, Avrami−Weibull function, expressed in the form: $y(t)/y_{max} = 1−\exp[(t/\Theta)^q]$ (where y_{max} is the maximum value of $y(t)$ when $t \to \infty$, and Θ and q are constants), is equally very versatile in explaining the generation rate $dy(t)/dt$ of items in terms of its parameters Θ and q. Using the basic concepts involved in the derivation of Avrami−Weibull function for overall crystallization from melt and supersaturated solution, the growth behavior of cumulative number $y(t)$ of items produced at time t by individual (simple) sources and collectives or groups of simple sources (i.e. complex or composite sources) is presented. Comparison of the process of receiving of citations by papers with the processes of occurrence of chemical reactions and crystallization of solid phases from melts and supersaturated solutions shows that this process is similar to that of overall crystallization of solid phases from melts and solutions. Analysis of growth of citations using Avrami−Weibull function to individual papers published by different authors shows that $1 < q < 4$ for most cases. This suggests that the process of citations to individual articles is mainly determined by progressive nucleation mode involving both diffusion and integration of published knowledge.

Keywords: Avrami−Weibull function; Gompertz and Verhulst functions; Growth behavior of items; Citation analysis

Streszczenie

Przeanalizowano i porównano stosowalność funkcji Avrami'ego−Weibulla, Verhulsta (logistycznej) i Gompertza do empirycznych danych sygmoidalnego przebiegu wzrostu $y(t)$ takich różnorodnych podmiotów jak: liczba artykułów i cytowań otrzymywanych przez pojedyncze i wszystkie kolejne artykuły publikowane przez wybranych wysoko cytowanych autorów, liczba kiełkowań nasion pomidorów i liczba trzech różnych bakterii. Zaobserwowano, że: 1) funkcja Avrami'ego−Weibulla opisuje różne dane lepiej niż funkcje Gompertza i Verhulsta, oraz 2) w porównaniu z funkcjami Verhulsta i Gompertza, funkcja Avrami'ego−Weibulla, wyrażona w postaci: $y(t)/y_{max} = 1−\exp[(t/\Theta)^q]$ (gdzie: y_{max} jest maksymalną wartością $y(t)$ gdy $t \to \infty$, oraz Θ i q są stałymi), jest równie wszechstronna w wyjaśnieniu szybkości wytwarzania $dy(t)/dt$ wyżej wymienionych podmiotów przy pomocy parametrów Θ i q. Korzystając z podstawowych pojęć zawartych w wyprowadzeniu równania Avrami'ego−Weibulla do opisania całkowitej krystalizacji z fazy roztopionej i z roztworu przesyconego, przedstawiono przebieg wzrostu kumulacyjnej liczby $y(t)$ podmiotów wytwarzanych w czasie t poprzez pojedyncze (proste) źródła i zbiory lub grupy pojedynczych źródeł (tj. złożonych źródeł). Porównanie procesu otrzymywania cytowań przez artykuły z procesami występowania reakcji chemicznych i krystalizacji ciał stałych ze stopów i roztworów przesyconych pokazuje, iż proces ten jest podobny do całkowitej krystalizacji ciał stałych ze stopów i roztworów. Analiza wzrostu cytowań według równania Avrami'ego−Weibulla pojedynczych artykułów publikowanych przez różnych autorów pokazuje, że w większości przypadków $1 < q < 4$. Z powyższego można wnioskować, że proces cytowania pojedynczych artykułów zachodzi w głównej mierze przez zarodkowanie progresywne oparte na dyfuzji i integracji opublikowanej wiedzy.

Słowa kluczowe: Funkcja Avrami'ego−Weibulla; Funkcje Gompertza i Verhulsta; Przebieg wzrostu podmiotów; Analiza cytowań

*Corresponding author (Emeritus Professor).

Email address: **k.sangwal@pollub.pl** (K. Sangwal)

1. Introduction

Since the World War II the scientific literature has witnessed steady growth of scientific research due to its increasing scope and volume. As measures of growth of the scientific literature one can mention the number of authors working in different scientific fields, the number of articles published in different fields, the number of journals published in different scientific disciplines, the number of papers published in individual journals, and the number of journals published in individual countries. Three types of growth of cumulative number $y(t)$ of items with time t are observed: (1) *normal* S-shaped plots with initial convex curvature followed by concave curvature, (2) *inverse* S-shaped plots with initial concave curvature followed by convex curvature, and (3) linear plots of $y(t)$ data. In order to describe the growth behavior of the above type of plots a variety of mathe-

matical functions involving empirical parameters have been developed and applied over years [1−8]. Among the different equations to describe the growth behavior of various phenomena, power-law, exponential and logistic (also called Verhulst's) functions are commonly used but Gompertz' function has also been reported [2].

In his classic work, Price [1] observed that in many cases the growth of science follows exponential dependence. In a detailed study devoted to the analysis of 20 different databases in humanities, social sciences, and science and technology (Sci-Tech), Egghe and Ravichandra Rao [2] found that the power-law function with an exponent greater than 1 is the best for Sci-Tech databases, whereas Gompertz' function, which is a generalization of exponential function, is the best to describe the growth of social sciences and humanities databases. Gupta et al. [4] applied selected functions to the data of cumulative growth of publications in six sub-disciplines of social sciences in the world and found that the power-law and logistic functions are the best to describe the growth of publications in the above sub-disciplines. Ravichandra Rao and Srivastava [5] analyzed the growth of journals, articles and authors in malaria research for the period 1955–2005 and found that the exponential function best fits the data. Wong and Goh [6] applied three competing growth functions, namely, simple logistic growth function, bi-logistic growth function and logistic function within a dynamic carrying capacity (LGDCC) to explain the growth behavior of the number of publications and patents of South Korea, Taiwan, Japan and Malaysia. These authors found that the bi-logistic growth function is the best for the number of publications as well as the number of patents of South Korea and Taiwan, the LGDCC function for the number of publications and the bi-logistic growth function for the number of patents of Japan, whereas the LGDCC for the number of publications and simple growth function for the number of patents of Malaysia.

Description of growth of a scientific phenomenon using mathematical functions is important for understanding their course in terms of the parameters of the functions and for predicting future trends. The values of the parameters of different functions are especially important for understanding the cause-and-effect relationship of the course of the phenomena. However, apart from fitting empirical data using various mathematical functions, sometimes erroneously called modeling [3,4], in the informetric literature there are several studies devoted to the statistical modeling of citation behavior of publications of individual authors [9-15] and to the theoretical development of statistical formulas for citation distribution [16,17]. In these models, the papers published by an author and the citations received by the papers are generated according to some statistical function. For example, in his stochastic model, Burrell [9-12] assumed that: (1) papers are published by an author according to a Poisson process at a constant rate, (2) citations to a paper are received according to a Poisson process at a constant rate, and (3) citation rate of the papers for the author varies according to gamma distri-

bution. In order to describe the time dependence of growth of cumulative citations of papers published by an author, Hirsch [18] proposed a deterministic model based on stretched exponential with exponent $q \leq 1$ (see Eq. (13)). In the case of a researcher publishing a constant number of papers and each paper fetching a fixed number of citations per year every subsequent year, stochastic and deterministic models predict approximately quadratic growth of the total number of his/her citations with publication time [11,18].

Application of various mathematical functions is not confined to describe growth of scientific literature alone. For example, logistic function and its modifications, Gompertz function and its modifications, and standard Avrami−Weibull function have been used in diverse areas such as various bacterial growth in different media (for example, see: refs. [19-30]), population growth of individual biological species (for example, see: ref. [31]), growth of Tumor cells [32,33], germination of seeds [34], and overall crystallization of various compounds (for example, see: [35-37]). However, among these functions, Avrami−Weibull function has been applied for the data analysis in relatively few studies [19,24,27,36,38]. In these studies this function is referred to as Weibull function.

The aim of the present study is two-fold: (1) to compare best fits of data of the growth behavior of different types of items by Avrami−Weibull, Verhulst and Gompertz functions, and (2) to analyze the growth of cumulative papers $N(t)$ by an author and cumulative citations $L(t)$ of his/her individual as well as progressively published papers, with special emphasis on their sigmoidal-shaped growth, as a function of time t using Avrami−Weibull function. Since the two fitting parameters of the Avrami−Weibull function as used in overall crystallization have well-defined physical interpretation, an additional aim of the study is to demonstrate that the process of growth of scientific literature is similar to overall crystallization from melts and solutions but differs fundamentally from chemical reactions described by chemical kinetics. The general concepts of occurrence of chemical reactions and formation of crystallization nuclei are briefly presented.

In the paper the following topics are discussed: (1) presentation of standard Avrami−Weibull, Verholst and Gompertz equations for the growth of items with time, (2) analysis of growth of different phenomena using Avrami−Weibull, Verholst and Gompertz functions in order to compare best fit of the data and then using Avrami−Weibull function examination of the effect of external factors on the growth of these phenomena, (3) description of basic concepts involved in the generation of items and their growth as a function of time in the form of Avrami−Weibull function, (4) predictions of Avrami−Weibull function on the growth and growth rate behavior of citations of papers in relation to changes in its parameters Θ and q and their confrontation with the empirical data of the dependence of yearly citations of all successively published papers and four individual top-cited papers of two highly-cited authors, and (5)

summary of the main findings of the study. Moreover, in order to introduce the reader to the topics discussed in the paper rudiments of occurrence of chemical reactions and crystallization, basic concepts of overall crystallization and comparison of predictions of different functions are briefly described in Appendices A, B and C, respectively.

2. Relevant mathematical functions

In order to describe the S-shaped curves observed for different phenomena we selected Avrami−Weibull, Verhulst (logistic) and Gompertz functions relating the growth of cumulative number $y(t)$ of items with time t. According to the Avrami−Weibull function the relationship between $y(t)$ and t is given by (for example, see: refs. [27,39,40])

$$y(t) = y_{max}\left\{1 - \exp\left[-\left(\frac{t}{\Theta}\right)^q\right]\right\}, \qquad (1)$$

where y_{max} is the value of $y(t)$ when $t \rightarrow \infty$, and Θ and q are constants. The constants Θ and q are called the location and shape factors, respectively [27].

According to the Verhulst (logistic) function the cumulative number $y(t)$ of items is of the form (for example, see: refs. [2,22,23,25,41,42])

$$y(t) = \frac{y_{max}}{1 + \left(\frac{y_{max}}{y_0} - 1\right)\exp(-\beta t)}, \qquad (2)$$

where y_0 is the number of items at $t = 0$, the maximum number of items y_{max} is the so-called carrying capacity, and β is the so-called Malthusian instantaneous growth rate parameter. According to the Gompertz function the relationship between $y(t)$ and t is given by (for example, see: [2,42-44])

$$y(t) = y_{max}\left\{1 - \exp\left[-\frac{\lambda}{c}(\exp ct - 1)\right]\right\}, \qquad (3)$$

where λ and c are fitting parameters.

For situations when $t \ll \Theta$, Avrami−Weibull equation (1) takes the power-law form:

$$y(t) = y_{max}\left(\frac{t}{\Theta}\right)^q, \qquad (4)$$

which takes a linear form when $q = 1$. The notation "«" denotes that the time t is much smaller than the time constant Θ. Note that, for $ct \ll 1$, Gompertz function (3) reduces to the form of Avrami−Weibull function (1), i.e.

$$y(t) = y_{max}\{1 - \exp(-\lambda t)\}. \qquad (5)$$

when $q = 1$ and $\lambda = 1/\Theta$. For $\lambda t \ll 1$, Eq. (5) reduces to the linear form of Eq. (4).

The above functions (1), (2) and (3) of growth of cumulative number $y(t)$ of items with time t describe cumulative distribution function $F(t) = y(t)/y_{max}$ and frequency density function $f(t) = dF(t)/dt =$

$[dy(t)/dt]/y_{max}$, where y_{max} is the maximum number (saturation limit) of items. These functions represent original versions of the three models and the differential $dy(t)/dt$ may be considered as rate of growth of $y(t)$ items whereas $[dy(t)/dt]/y_{max}$ as dimensionless rate. As mentioned in the Introduction, various modified versions of Verhulst (logistic) and Gompertz models have been proposed in the literature to explain real $y(t)$ data satisfactorily but until now the Avrami−Weibull function has been used in its original version. It is beyond the scope of this paper to discuss the modified versions of different models.

3. Analysis of growth behavior of different items

The growth data were analyzed using commercially available "Origin 9.1" package. This package employs nonlinear least-squares fitting of the data and yields values of the fitting parameters of an equation, their standard deviations, chi-square (χ^2) residual and the corresponding goodness-of-the-fit parameter R_y^2.

For the analysis we used typical examples of data on the cumulative growth of papers and citations earned by individual and all successively published papers, up to 2013, of selected top-cited authors reported by Chuang and Ho [45] and data on the growth behavior of different phenomena such as germination of seeds, three different bacteria, and overall crystallization of polypropylene. The basic bibliometric data of the selected authors comprised cumulative number $N(t)$ of papers of J. Felsenstein, cumulative number $L(t)$ of citations received by two top-cited papers of D.R. Cox and cumulative number $L(t)$ of citations received by four top-cited papers and by all papers published by U.K. Laemmli, taking publication and citation duration $t = Y−Y_0$, with Y and Y_0, as the years corresponding, respectively, to t and $t = 0$. The data were collected during 20-25 October 2014 from the Thomson Reuters' Web of Knowledge database. The growth data on the other phenomena were collected from the published literature.

3.1. Some specific examples of growth behavior of items and their analysis by different functions

Figures 1a and 1b show examples of the plots of cumulative number $N(t)$ of papers of Felsenstein and cumulative number $L(t)$ citations of top-cited papers of Cox with time t, respectively, exhibiting S-shaped curves. In the figures solid, dashed and dotted curves are drawn according to Avrami−Weibull, Verhulst and Gompertz functions, respectively, with the best-fit values of parameters given in Tables 1−3.
From the values of goodness-of-the-fit parameter R_y^2 listed in these tables it may be noted that Avrami−Weibull function fits the data better than Verhulst and Gompertz functions. As seen from the best-fit plots of the data according to Verhulst function (2), noticeable deviations in the fit of the data are encountered in the initial and later stages. However, the fit improved when
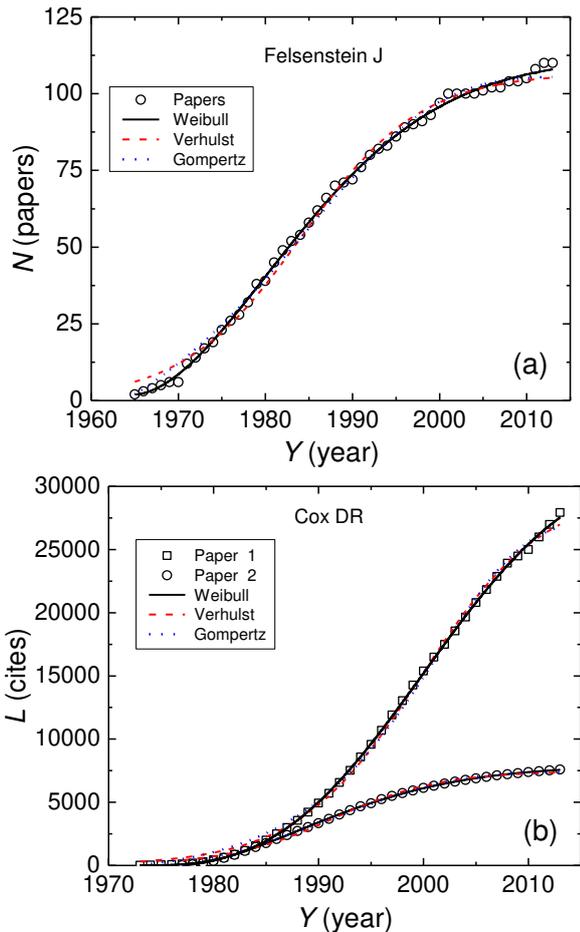
Figure 1: Example of evolution of (a) cumulative number $N(t)$ of papers of Felsenstein and (b) cumulative number $L(t)$ citations of top-cited papers of Cox with time t showing S-shaped curves. Solid, dashed and dotted curves represent plots according to Avrami−Weibull, Verhulst and Gompertz functions, respectively, with the best-fit values of parameters given in Tables 1−3.

the initial $y(t)$ corresponding to Y_0 was taken as $C > 0$ (see Tables 2 and 3).

Figure 2 illustrates a typical example of the plots of cumulative number $L(t)$ of citations of all progressively published papers and the top-cited paper of Laemmli with time t showing S-shaped curves. As in Figure 1, solid, dashed and dotted curves represent plots according to Avrami−Weibull, Verhulst and Gompertz functions, respectively, with the best-fit values of parameters given in Tables 1−3. The last three steeply rising points of the data beyond the arrow were excluded from analysis.

The values of the goodness-of-the-fit parameter R_y^2 given in Tables 1−3 again show that Avrami−Weibull function fits the data better than Verhulst and Gompertz functions which show similar R_y^2 parameter. As in the plots of Figure 1, noticeable deviations in the plots are encountered in the initial and later stages of the data.

Figure 3 shows the evolution of germination of cumulative number $N(t)$ of unirradiated and irradiated tomato seeds at 15 °C with time t. Solid, dashed and dotted curves represent plots according to Avrami−Weibull, Verhulst and Gompertz functions, respectively,

with the best-fit values of parameters given in Tables 1−3. As seen from the values of the R_y^2 parameter, the $N(t)$ data are best described by Avrami−Weibull function but worst by Verhulst function. This poor fit is mainly due to the fact that, apart from large deviations from the fit at $t > 200$ h, according to this relation $N_0 > 0$ at $t = 0$ but according to the original $N(t)$ data $N_0 = 0$.
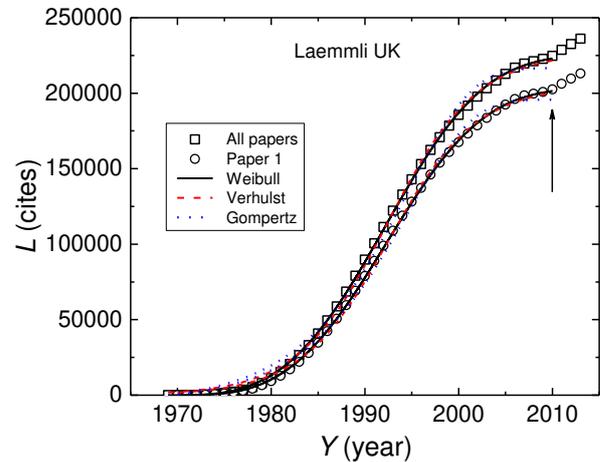

Figure 2: Example of evolution of cumulative number $L(t)$ of citations of all progressively published papers and the top-cited paper of Laemmli with time t showing S-shaped curves. Solid, dashed and dotted curves represent plots according to Avrami−Weibull, Verhulst and Gompertz functions, respectively, with the best-fit values of parameters given in Table 1. The last three points of the data were excluded from analysis.
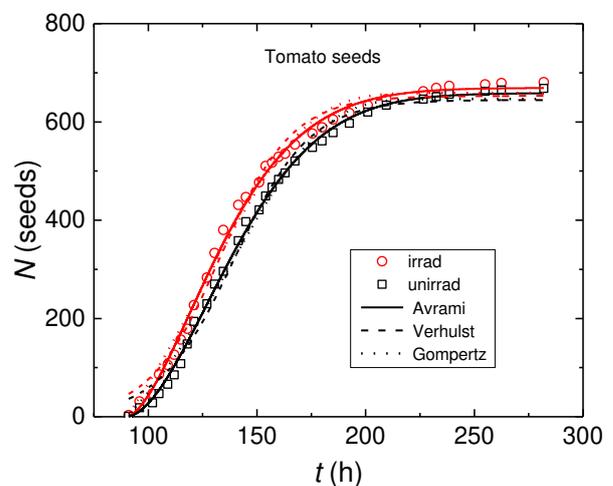

Figure 3: Evolution of germination of cumulative number $N(t)$ of unirradiated and irradiated tomato seeds at germination temperature $T = 15$ °C with time t showing S-shaped curves. Solid, dashed and dotted curves represent plots according to Avrami−Weibull, Verhulst and Gompertz functions, respectively, with the best-fit values of parameters given in Table 1. Original data from Gładyszewska [34].

The above examples show that Avrami−Weibull function (1), in general, describes different types of the data better than Gompertz and Verhulst functions. Keeping in view the fact that Avrami−Weibull relation (1) describes the time dependence of cumulative citations $L(t)$ received by individual papers better than the other two functions, the $L(t)$ data of three subsequently

Table 1: Values of parameters of Verhulst equation (2)

Data	Source	y_{max}	y_0	β	t_0	χ^2	Ry^2
$N(t)$	Felsenstein, papers	106.8	6.62	0.1459	1965 yr	7.163	0.9947
$L(t)$	Cox, paper 2	7461	414.1	0.1963	1977 yr	35809	0.9947
	Cox, paper 1	29798	314.6	0.1700	1973 yr	151915	0.9983
	Laemmli, paper 1	204971	1662	0.2134	1970 yr	$7.3730\cdot10^6$	0.9987
	Laemmli, all papers	227048	1680	0.2096	1969 yr	$1.0013\cdot10^7$	0.9986
$N(t)$	Tomato, 15°C, unirr[a]	644.8	34.63	0.0577	90 h	494.41	0.9909
	Tomato, 15°C, irr[a]	653.0	43.73	0.0609	90 h	566.76	0.9892

[a] Abbreviations: unirr – unirradiated; irr – irradiated; Tomato – tomato seed germination.

Table 2: Values of parameters of Gompertz equation (3)

Data	Source	C	y_{max}	$10^3\lambda$	10^2c	t_0	χ^2	Ry^2
$N(t)$	Felsenstein, papers	2	103.6	17.23	6.87	1965 yr	5.595	0.9958
$L(t)$	Cox, paper 2	23	7391	24.23	8.73	1977 yr	14515	0.9978
	Cox, paper 1	9	27189	3.53	12.49	1973 yr	229894	0.9975
	Laemmli, paper 1	4	195749	3.88	14.72	1970 yr	$2.282\cdot10^7$	0.9962
	Laemmli, all papers	2	216577	3.50	14.57	1969 yr	$3.021\cdot10^7$	0.9959
$N(t)$	Tomato, 15°C, unirr[a]	0	646.6	7.14	2.46	90 h	432.75	0.9920
	Tomato, 15°C, irr[a]	0	658.8	9.69	2.20	90 h	482.23	0.9908

[a] Abbreviations: unirr – unirradiated; irr – irradiated; Tomato – tomato seed germination.

Table 3: Values of parameters of Avrami−Weibull equation (1)

Data	Source	C	y_{max}	Θ	q	t_0	χ^2	Ry^2
$N(t)$	Felsenstein, papers	2	109.7	24.2 yr	1.766	1965 yr	1.591	0.9988
$L(t)$	Cox, paper 2	23	7864	18.2 yr	1.706	1977 yr	607.2	0.9999
	Cox, paper 1	9	31655	31.3 yr	2.888	1973 yr	16960	0.9998
	Laemmli, paper 4	1	963.5	16.4 yr	2.083	1971 yr	--	0.9997
	Laemmli, paper 3	16	3743	17.4 yr	1.784	1974 yr	--	0.9983
	Laemmli, paper 2	16	5670	11.2 yr	1.667	1977 yr	--	0.9996
	Laemmli, paper 1	4	203935	25.2 yr	3.193	1970 yr	$8.7679\cdot10^5$	0.9998
	Laemmli, all papers	2	225782	26.0 yr	3.258	1969 yr	$1.5617\cdot10^6$	0.9998
$N(t)$	Tomato, 15°C, unirr[a]	0	658.5	60.0 h	1.758	90 h	91.20	0.9983
	Tomato, 15°C, irr[a]	0	669.1	53.2 h	1.614	90 h	157.35	0.9970

[a] Abbreviations: unirr – unirradiated; irr – irradiated; Tomato – tomato seed germination.

top-cited papers (i.e. papers 2, 3 and 4) were analyzed by using Eq. (1). The best-fit parameters for these data are included in Table 3. It is interesting to note that the values of the time constant Θ and the exponent q differ widely among the individual papers but their values for the combined cumulative $L(t)$ citations of all papers are higher than those for the citations of individual papers. This observation is consistent with the modeling of items in a previous paper [39].

The above analysis shows that Avrami−Weibull function (1) can be used to describe the data of growth behavior of both abstract (imaginary) items such as papers published by an author and citations received by his/her individual and all successively published papers as well as material (real) items such as germination of seeds and bacteria.

3.2. Effect of temperature on the growth behavior of material items

Every plot of the growth of cumulative number $y(t)$ of items against time t is characterized by three parameters: dimensionless growth rate $R = dy/y_{max}dt$ determined from the linear part of a $y(t)/y_{max}$ plot, time lag t_0 corresponding to the onset of initial growth, and time constant Θ when the rate R reaches a maximum value. In the case of growth of material items such as bacteria, it is usually observed that the growth rate R increases

whereas the time lag t_0 and the time constant Θ decrease with increasing temperature T. Some typical examples of the effect of temperature on these parameters are presented below.
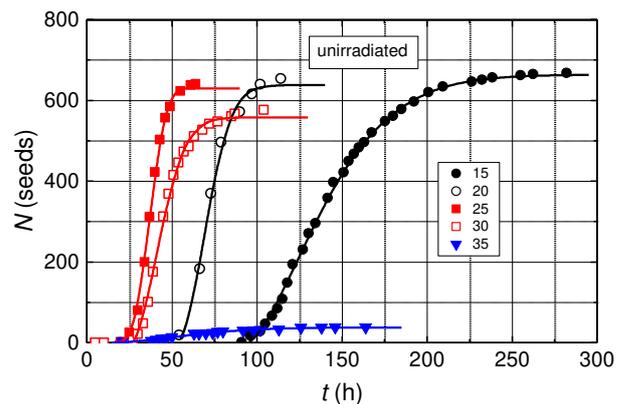

Figure 4: Evolution of germination of cumulative number $N(t)$ of unirradiated tomato seeds at different T with time t showing S-shaped curves. Curves represent plots according to Avrami−Weibull function with the best-fit values of parameters given in Table 1. Original data from Gładyszewska [34].

Figure 4 shows, as an example, the evolution of germination of cumulative number $N(t)$ of unirradiated tomato seeds at different temperature T with time t

showing S-shaped curves. Germination temperature T given in the figure is in $^{\circ}$C. Curves represent plots according to Avrami−Weibull function (1) with the best-fit values of parameters given in Table 4. A similar behavior was observed in the case of germination of irradiated seeds by specific dose of γ radiation. The best-fit parameters for these data are included in Table 4.

It may be seen from Table 4 that, irrespective of the initial irradiation treatment, at every germination temperature there is a time lag t_0 for germination. With an increase in temperature, this time lag t_0 shows a general decreasing trend. The time constant Θ also shows a similar decreasing trend up to 30 $^{\circ}$C and then it increases to a high value at 35 $^{\circ}$C. In contrast to the trends of time lag t_0 and time constant Θ, the exponent q initially increases from a relatively low value at 15 $^{\circ}$C, then attains a maximum at 25 $^{\circ}$C and subsequently at 35 $^{\circ}$C decreases to a value even lower than that at 15 $^{\circ}$C.

Table 4: Values of parameters N_{max}, Θ, q and t_0 of Avrami−Weibull equation for $N(t)$ data of tomato seed germination

Sample[a]	T ($^{\circ}$C)	N_{max}	Θ (h)	q	t_0 (h)
Unirradiated	15	658.5	60.06	1.758	90
	20	635.6	25.03	2.291	50
	25	629.5	24.66	3.611	15
	30	557.5	21.80	1.874	26
	35	37.8	57.07	1.720	15
Irradiated	15	669.1	53.17	1.614	90
	20	682.1	23.17	1.626	50
	25	660.9	22.90	3.448	15
	30	559.4	27.00	2.328	20
	35	73.6	61.29	1.103	5

Examination of the plots of the germination of both unirradiated and irradiated cumulative number $N(t)$ of seeds as a function of germination time t reveals that the seed germination rate $R = dN/N_{max}dt$, determined from the linear parts of the $N(t)$ plots, initially increases from a relatively low value at 15 $^{\circ}$C, then attains a maximum at 25 $^{\circ}$C and subsequently at 35 $^{\circ}$C decreases to a value even lower than that at 15 $^{\circ}$C. This trend is similar to that followed by the temperature dependence of the exponent q.

The effect of temperature on time lag t_0 and time constant Θ is not confined to germination of tomato seeds alone. The effect of temperature is observed, among others, on various bacterial growth in different media (for example, see: refs. [19-23, 25-30]), and population growth of individual biological species (for example, see: ref. [31]).

Data on the parameters Θ and q of Avrami−Weibull function for two toxin-producing *Bacillus cereus* (BC) and *Escherichia coli* (EC) microorganisms in carrot broth obtained at different temperatures have been reported by Fernandez et al. [19] and Aragao et al. [27], respectively. From these studies one observes that Θ decreases with an increase in temperature in the temperature range investigated in the growth of the microorganisms. However, the values of q suggest that it is independent of temperature. These trends of Θ and q are

somewhat different from those observed in the case of germination of tomato seeds.

Growth behavior of various bacteria in different media under different experimental conditions such as temperature and pH has been analyzed in several studies using different functions [21,23,29,30]. In these studies microorganism cell concentration at time t, concentration at $t = 0$, and their maximum concentration, denoted by $y(t)$, y_0 and y_{max}, respectively, in Eqs. (1)-(3), are customarily expressed in log(cfu mL^{-1}). Examination of the data of the growth rates $R = dy/y_{max}dt$ of various microorganisms grown at different temperatures shows that their value increases with increasing temperature and that, at a particular temperature, the rate R is frequently inversely related to the time lag t_0, with a proportionality constant K characteristic of the bacteria−medium system, which lies between 1 and 3 (cf. refs. [21,29]). In the case of tomato seeds this inverse relationship between time lag t_0 for germination and growth rate R is observed up to 25 $^{\circ}$C. Obviously, here the trend at temperatures of 30 and 35 $^{\circ}$C is anomalous. A possible explanation of this anomalous trend in the germination of tomato seeds is associated with differences in the kinetics of *testa* and *endosperm* ruptures during germination [46,47].

We assume that the dependence of germination rate R of tomato seeds in the sand and growth rates R of microorganisms in different media are instances of chemical reactions with reaction rate constants k described by Arrhenius-type relation (A3) and that the time lag t_0 and time constant Θ for germination of tomato seeds and growth of microorganisms are inversely proportional to the reaction rate constant k with a proportionality constant K. Then from Eq. (A3) the dependence of rate constant k, and time lag t_0 and time constant Θ on temperature T, taken in Kelvin, may be described by

$$\ln k = \ln A - \frac{\Delta G_R^0}{R_G T} , \qquad (6)$$

$$\ln t_0, \Theta = \ln\left(\frac{K}{A}\right) + \frac{\Delta G_R^0}{R_G T} , \qquad (7)$$

respectively. Here ΔG_R^0 is the energy difference between reactants and products, all in their respective ground states, A is the frequency factor, and R_G is the gas constant. These relations predict linear dependences between $\ln k$ or $\ln t_0, \Theta$ and $1/T$, with intercept $\ln k$ or $\ln(K/A)$ and slope $\Delta G_R^0/R_G$, which enables to calculate frequency factor A or relative frequency factor A/K and activation energy ΔG_R^0 for the reaction.

Figure 5a shows the dependence of growth rate R, taken as a measure of rate constant k, of different bacteria on temperature T according to relation (6). To facilitate a comparison of the trends of the dependence according to Eq. (6) with those of the dependence of $\ln t_0$ and $\ln \Theta$ on $1/T$ according to Eq. (7), the $R(T)$ data are shown as plots of $-\ln R$ against $1/T$. The original data for *Listeria monocytogenes* (LMC) in 2% milk and 12 and

30% milk creams are from Lobacz and Kowalik [30], for *Yersinia enetrocolitica* in Camembert-type cheese from Kowalik and Lobacz [29], for *Bacillus cereus* AVTZ415 (BC 415) and AVZ421 (BC 421) in nutrient carrot broth and for *Bacillus cereus* AVTZ415 (BC 415) in natural carrot broth from Valero et al. [21], and for *Escherichis coli* (EC) in nutrient broth from Fujikawa et al. [23]. In view of large scatter in the values of R for LMC in different samples of milk cream and for BC in different broths the data for LMC in 12% milk cream and BC 415 in neutral carrot broth were fitted according to Eq. (6) with the best-fit values of intercept $\ln A$ and slope $\Delta G_R^0/R_G$ listed in Table 5. The values of A and ΔG_R^0 calculated from the above parameters are included in the table.

Figure 5b illustrates the plots of $\ln t_0$ for germination of unirradiated and irradiated tomato seeds and for growth of different bacteria as a function of $1/T$ according to Eq. (7). The data of time lag t_0 for the germination of tomato seeds were obtained from the original cumulative $N(t)$ data reported by Gładyszewska [34] using Avrami−Weibull (AW) function (present author) and Verhulst/logistic) (V/log) function by Gładyszewska [34], whereas those for the growth of *Listeria mono-cytogenes* (LMC) in milk are from Lobacz and Kowalik [30], for *Yersinia enetrocolitica* (YE) in Camembert-type cheese from Kowalik and Lobacz [29], and for *Bacillus cereus* AVTZ415 (BC 415) and AVZ421 (BC 421) in nutrient carrot broth and for *Bacillus cereus* AVTZ 415 (BC 415) in natural carrot broth from Valero et al. [21]. For tomato germination and bacteria growth in carrot broth linear plots are drawn for the data obtained by Avrami−Weibull function of unirradiated tomato seeds and for *Bacillus cereus* AVTZ415 with the best-fit values of intercept $\ln(K/A)$ and slope $\Delta G_R^0/R_G$ given in Table 5. The calculated values of A/K and ΔG_R^0 for different growths are also listed in Table 5.

Figure 5c shows the dependence of time constant Θ for growth of three different bacteria on temperature T according to Eq. (7). The original data for *Bacillus cereus* AVTZ415 (BC 415) and AVZ421 (BC 421) in neutral carrot broth are taken from Fernandez et al. [19] and for *Escherichis coli* (EC) in nutrient broth are from Aragao et al. [27]. The best-fit plots of the data according to relation (7) are drawn with the values of intercept $\ln(K/A)$ and slope $\Delta G_R^0/R_G$ listed in Table 5. From these best-fit parameters the calculated values of A/K and ΔG_R^0 are included in Table 5.

From Table 5 it may be noted that the value of ΔG_R^0 for bacteria like *Bacillus cereus* AVTZ415 and *BC* AVZ421 in carrot broth, *Listeria monocytogenes* in milk and *Yersinia enerocolitica* in Camembert-type cheese increases in the sequence: $R(t)$, $t_0(T)$ and $\Theta(T)$ data, whereas the value of A and A/K for them increases in the sequence: $t_0(T)$, $R(t)$ and $\Theta(T)$ data. The values of ΔG_R^0 and A (or A/K) corresponding to a particular growth parameter such as growth rate R or time lag t_0 vary enormously among different samples. For example,
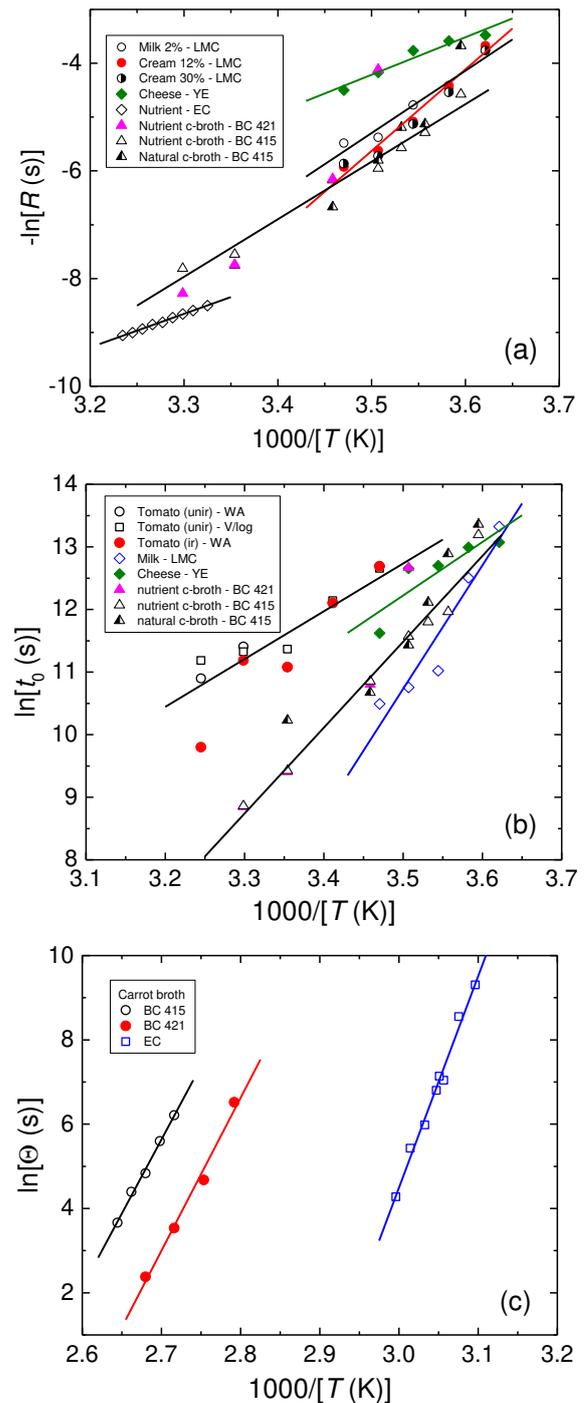

Figure 5: Dependence of (a) dimensionless growth rate R of different bacteria on temperature T according to relation (6), and (b) time lag t_0 for growth of different items and (c) time constant Θ for the growth of three different bacteria in carrot broth on temperature T according to relation (7). For the purpose of comparison with the $t_0(T)$ and $\Theta(T)$ data according to Eq. (8), in (a) data of growth rate $R(T)$ are presented as $-\ln R$. See text for details.

the values of ΔG_R^0 obtained from the $R(T)$ data are relatively low for the growth of *Escherichis coli* in nutrient broth and *Yersinia enerocolitica* bacteria in Camembert-type cheese and in comparison with that for the growth of *Listeria monocytogenes* in milk products. Similarly, the value of ΔG_R^0 obtained from $t_0(T)$ data is relatively

Table 5: Parameters of Eqs. (6) and (7) from $R(T)$, $t_0(T)$ and $\Theta(T)$ data

Data	Sample	Medium	$-\ln A$, $\ln(K/A)$	$10^3 \Delta G_R^0/R_G$ (K)	A, A/K (s^{-1})	ΔG_R^0 (kJ/mol)	Ry^2	Ref.
$R(T)$	BC AVT415, AVTZ421	Nutrient c-broth	-43.25	10.69	$6.1 \cdot 10^{18}$	88.9	0.9754	[21]
	BC AVT415	Natural c-broth	-43.25	10.69	$6.1 \cdot 10^{18}$	88.9	0.9754	[21]
	E Coli	Nutrient c-broth	-29.18	6.22	$4.7 \cdot 10^{12}$	51.7	0.9974	[23]
	L-monocytogenes	UHT milk 2%	-45.82	11.58	$7.9 \cdot 10^{19}$	96.3	0.9473	[30]
		UHT cream12%	-58.65	15.15	$3.0 \cdot 10^{25}$	126.0	0.9744	[30]
	Y-enterocolitica[a]	Cheese	-28.57	6.96	$2.6 \cdot 10^{12}$	57.9	0.9249	[29]
$t_0(T)$	Tomato seeds	Soil	-14.0	7.64	$1.2 \cdot 10^6$	61.3	0.7715	[34]
	BC AVT415, AVTZ421	Nutrient c-broth	-36.53	13.72	$7.3 \cdot 10^{15}$	114.1	0.9744	[21]
	L-monocytogenes	UHT Milk	-58.37	19.74	$2.2 \cdot 10^{25}$	164.1	0.8829	[30]
	Y-enterocolitica[a]	Cheese	-17.65	8.54	$4.6 \cdot 10^7$	71.0	0.6938	[29]
$\Theta(T)$	BC AVTZ421	Nutrient c-broth	-89.06	35.07	$4.8 \cdot 10^{38}$	291.1	0.9937	[19]
	BC AVT415	Nutrient c-broth	-95.01	36.30	$1.8 \cdot 10^{41}$	301.8	0.9808	[19]
	E Coli	Culture c-media	-146.05	50.18	$2.7 \cdot 10^{63}$	417.2	0.9846	[27]

low for the germination of tomato seeds and for the growth of *Yersinia enerocolitica* bacteria in Camembert-type cheese in comparison with that for the growth of *Listeria monocytogenes* in milk products. From these results it may be concluded that, for a particular bacterial growth, the differences in the values of ΔG_R^0 and A obtained from $R(T)$ data from those of ΔG_R^0 and A/K from $t_0(T)$ and $\Theta(T)$ data are due to different processes associated with them.

3.3. Overall crystallization of various compounds

Overall crystallization of compounds from melts and solutions also exhibits features similar to those of growth of material items discussed above. However, in this case, the plots of growth of overall crystallization are presented in terms of cumulative mass $y(t)$ of the crystallized compound instead of cumulative number $y(t)$ of material items against time t. These $y(t)$ plots are also characterized by three parameters: dimensionless growth rate $R = dy/y_{max}dt$, time lag t_0, and time constant Θ.

The process of overall crystallization of a compound involves the formation of stable nuclei and their subsequent development to visible dimensions in the bulk medium (see Appendix B). Both of these processes depend, among others, on crystallization temperature (for example, see: refs. [35-37]). Figure 6 illustrates a typical example of the dependence of overall crystallization fraction $y(t)/y_{max}$ of polypropylene on time t at different crystallization temperatures. Original data of the figure are from Lopez-Manchado et al. [48] but best-fit curves are drawn by Padar et al. [36], according to Avrami−Weibull function (1) assuming the initial time $t_0 = 0$ for the onset of overall crystallization. It may be noted that the best-fit plots somewhat deviate from the experimental data points at low and high crystallization times. These deviations are mainly associated with the assumption that $t_0 = 0$ [37]. The experimental data reveal that the initial time t_0 when crystallization fraction begins to increase is not zero and increases with increasing crystallization temperature.

The crystallization rate $R = dy/y_{max}dt$ of polypropylene, determined from the linear part of the $y(t)/y_{max}$ plots

at a particular temperature, decreases with an increase in crystallization temperature T. According to Arrhenius-type relation (A3), the higher the reaction temperature T, the higher is the value of the reaction rate constant k. This inference is contrary to the dependence of crystallization rate $R = dy/y_{max}dt$ of polypropylene on crystallization temperature T (Figure 6). Therefore, unlike the cases of temperature dependence of cumulative growth of germination of tomato seeds and growth of microorganisms discussed above, Arrhenius-type relation (A3) does not describe the dependence of time lag t_0 for crystallization from melts on T.
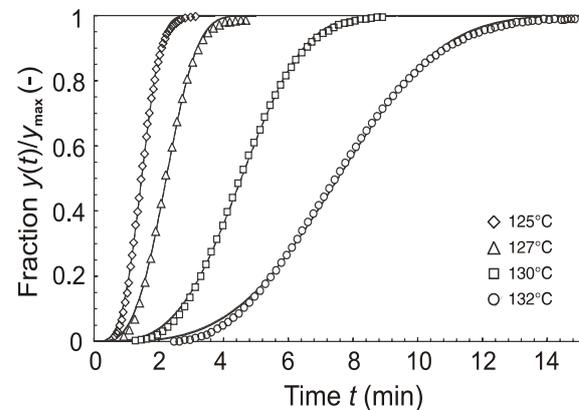

Figure 6: Example of dependence of overall crystallization fraction $y(t)/y_{max}$ of polypropylene on time t at different crystallization temperature. Solid curves represent plots according to Avrami−Weibull function. Original data from Lopez-Manchado et al. [48] but best-fit plots are drawn by Padar et al. [36]. Adapted from Padar et al. [36].

Figure 6 shows that the crystallization rate R is related to the corresponding time lag t_0 in the plots. The lower the crystallization rate at a particular temperature T, the higher is the value of the time lag t_0 for detectable crystallization. There is also a similar relationship between R and time constant Θ. In order to explain the temperature dependence of crystallization rate R, time lag t_0 and time constant Θ for crystallization from melts on T, one uses Eq. (A10) and assumes that $R = K_1 J$, and t_0 and $\Theta = K_2/J$, where K_1 and K_2 are new proportionality constants different from K. Then from Eq. (A10) one obtains

$$\ln R = \ln(K_1 J_0) - \frac{B'}{T(\Delta T)^2} , \qquad (8)$$

and

$$\ln t_0, \Theta = \ln\left(\frac{K_2}{J_0}\right) + \frac{B'}{T(\Delta T)^2} , \qquad (9)$$

where B' is given by Eq. (A11), and the temperature difference $\Delta T = (T_m - T)$, with T_m as the melting point of the crystallizing compound. Eqs. (8) and (9) predict B' > 0 because the main contribution to R and t_0 or Θ comes from ΔT rather than from T.
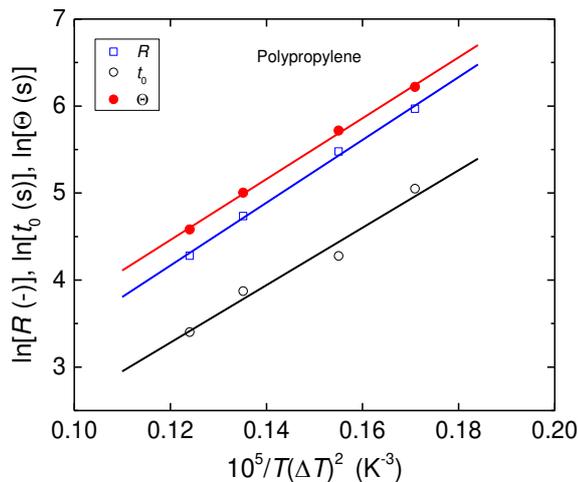

Figure 7: Plots of $-\ln R$, $\ln\Theta$ and $\ln t_0$ against $1/T(\Delta T)^2$ for crystalization of polypropylene according to Eqs. (8) and (9). For the purpose of comparison with the $t_0(T)$ and $\Theta(T)$ data according to Eq. (8), data of crystallization rate $R(T)$ are presented as $-\ln R$. See text for detail.

Table 6: Parameters of relation (A10) from $R(T)$, $t_0(T)$ and $\Theta(T)$ data of crystallization of polypropylene

Data	$-\ln J_0$, $\ln(K'/J_0)$	$10^5 B'$ (K^3)	J_0, J_0/K' (s^{-1})	Ry^2
$R(T)$	−0.168	36.1	1.18	0.9955
$t_0(T)$	−0.684	33.0	1.98	0.9572
$\Theta(T)$	0.257	35.0	0.77	0.9980

Figure 7 presents the $R(T)$, $t_0(T)$ and $\Theta(T)$ data of crystallization of polypropylene ($T_m = 170\ ^o$C) from the melt according to relation (8) whereas the linear plots are drawn with the values of the parameters listed in Table 6. The $t_0(T)$ data were visually determined from the original plots of evolution of crystallization at different temperatures. The $R(T)$ data were recovered from the figure in the paper of Padar et al. [36] but the $\Theta(T)$ data were calculated from the values of best-fit constants q and Θ^{-q} reported in that paper. It may be noted from the table that the value of B' for the $R(T)$, $t_0(T)$ and $\Theta(T)$ data is essentially constant but the value of $\ln(K_2/J_0)$ for the $\Theta(T)$ data is higher than that for the $t_0(T)$ data. The constancy of B' is associated with the interfacial energy γ of the crystallites (see Eq. (A11)) but the different values of J_0/K_2 are associated with different sizes of the crystallites corresponding to t_0 and Θ. Obviously, the process of overall crystallization is

entirely different from the processes involved in bacterial growth discussed above.

3.4. Distinction between processes of chemical reactions and overall crystallization

The plots of the growth of cumulative number $N(t)$ of material items such as seeds (Figures 3 and 4) and the fraction of cumulative mass $y(t)/y_{max}$ of crystallized compounds (Figure 6) are similar and can be described reliably by Avrami–Weibull relation (1). However, the temperature dependence of rate R, time lag t_0 and time constants Θ for the growth of material items and overall crystallization of compounds differs fundamentally from each other. In the former cases the temperature dependence of these parameters can be described by Eqs. (6) and (7). These equations follow from the Arrhenius relation (A3) where the three parameters are related to the activation energy ΔG_R^0 involved in a reaction. However, in the latter case the temperature dependence of these parameters can be described by Eqs. (8) and (9). These relations follow from Eq. (A8) where the three parameters of crystallization are associated with the driving force ΔG_R. Obviously, the time lag t_0 for a phenomenon corresponds to an initial time period in which an equilibrium is attained in the system from the standpoint of occurrence of chemical reactions with rate k (see Eq. (A3)) or crystallization with nucleation rate J (see Eq. (A8)).

As discussed in Appendix B, the reaction rate constant k of a qth order chemical reaction and the time constant Θ of overall crystallization are mutually related by: $k = \Theta^{-q}$. Therefore, for overall crystallization occuring by instantaneous and progressive nucleation modes the relationships may be given by (see Appendix B)

$$k = \Theta^{-q} = \frac{\kappa g^q}{V} N_m , \qquad (10)$$

and

$$k = \Theta^{-q} = \frac{\kappa g^{q-1}}{q} J , \qquad (11)$$

which hold when $q \geq 0$ and $q \geq 1$, respectively.

From the above considerations it may be concluded that the processes associated with chemical reactions follow simple Arrhenius-type relation (A3) of the dependence of parameters R, t_0 and Θ on T with an activation energy ΔG_R^0, but those of overall crystallization follow relation (A8) in which the parameters R, t_0 and Θ are related to dependence of the number N_m of nuclei formed or the nucleation rate J on driving force ΔG_R.

4. Basic concepts about generation of abstract items

4.1. Motivation threshold for nucleation/growth of abstract items

The generation of *abstract* or *imaginary* items such as the number of papers and their citations is, by its nature, similar to a chemical reaction between the initial reactants involving the formation of an activated complex

followed by its dissociation into reaction products (for example, see [49]). It also has its analog in behavioral psychology as stipulated in the stimulus–response behavior theory involving attainment of a goal by human beings and animals through generation of inner tendency (i.e. restless or transition state) of the behaving organism, aroused by the external stimulus (see ref. [50]; Chapters 5 and 6). In this case, the ultimate goal is a consequence of decision making and is associated with the problem of motivation, a term "often used in reference to the conscious feeling of desire and the whole complex of ideas and feelings which together seem to constitute the conscious antecedents of behavior according to traditional wisdom" (ref. [50]; page 273).

It should be noted that the processes of chemical reactions and decision making differ from each other. The occurrence of chemical reactions is described in terms of thermodynamics but it is difficult to give a thermodynamic interpretation for the transition state involved in decision making. However, results of motivations of authors to cite published papers indeed reveal that there is always a cognitive pressure on authors towards citing a given paper and there is a threshold value of this cognitive pressure for the citation of a paper [51]. Threshold cognitive pressure on an author in citing previously published papers is equivalent to the free energy change ΔG_a involved in the formation of an activated complex X^* whereas cognitive pressure in citing is analogous to the total free energy change $\Delta G_a'$ associated with the dissociation of the activated complex X^* into the formation of reaction products (see Figure A1). Intuitionally, the process of citation of a paper P_{W1} of an author W1 by the citing author W2 in his/her paper P_{W2} bearing citation C_{W1} to the paper PW1 of author W1 may be represented in the form of the reaction (cf. Eq. (A1))

$$P_{W1} + W2 \to X^* \to P_{W2} + C_{W1} + \Delta G_R, \qquad (12)$$

with $\Delta G_a' = \Delta G_a + \Delta G_R$. Here $\Delta G_a'$, ΔG_a and ΔG_R of Fig. A1 now represent the overall, the threshold and the resulting cognitive citation pressures, respectively. The threshold cognitive pressure is the so-called motivation threshold for the citation of an article. Note that the resulting cognitive citation pressure ΔG_R is essentially associated with the attractiveness of the cited paper P_{W1}. The higher the attractiveness of this paper, the higher is its citability.

With the above information on the resulting cognitive citation pressure ΔG_R as the driving force for the citations received by a paper, we may apply the concepts of occurrence of chemical reactions and crystallization of solid phases from melts and supersaturated solutions to understand the process of citations of papers (see Appendix A). While applying Eq. (A3) to describe the occurrence of chemical reactions and Eq. (A8) to describe the process of nucleation of solid phase we ignore the role of temperature and assume it as a constant parameter. As seen from Eq. (A3), in the case of chemical reactions, the value of cumulative volume (reactant concentration), determined by reaction rate constant k, decreases with an increase in ΔG_R. In con-

trast to this, Eq. (A8) shows that, in the case of formation and growth of nuclei, the cumulative volume, determined by nucleation rate J, increases with an increase in ΔG_R. Therefore, it may be argued that the process of citations of papers is similar to that of overall crystallization of solid phases from melts and solutions and differs fundamentally from chemical reactions.

Citations to individual published articles of authors with time is a typical example of information production process. We use below the concepts of the occurrence of overall crystallization of solid phase to understand these processes of growth of *abstract* items.

4.2. Growth behavior of cumulative volume of abstract items

The time dependence of cumulative number of abstract items such as journals, articles and authors in a scientific field is a continuous information production process in which new items are produced progressively. An author publishing N papers in his research career and a research paper published by a given author receiving a total of L citations during its citation life are typical examples of closed systems. Here the author publishing N papers in his/her academic career and each ith paper receiving L_i citations are primary sources producing primary items (i.e. papers and citations, respectively). These source–items isolated systems are simple in nature because the source is an individual entity. However, when a group of primary items (for example, $N(t)$ papers published by the author in time t) act as secondary sources which produce cumulative secondary items (for example, cumulative number $L(t)$ of citations such that $L(t) = \Sigma L_i(t)$), one deals with complex or composite systems.

The processes of generation of primary items A from a source S and of secondary items B from primary items A acting as secondary sources of (secondary) items are schematically shown in Figure 8. In the figure cumulative number of primary and secondary items from individual primary and secondary sources are indicated by N and n, respectively. However, in general, when an individual source is not distinguished as primary or secondary source, the cumulative number of items is denoted by y.

In order to describe the time dependence of cumulative number y of primary items (e.g. papers) produced by a primary source (e.g. by an author) we may follow the concepts of overall crystallization of a solid phase occurring in a closed liquid system of fixed volume V. We make the following assumptions:

(1) Every source–items system is confined to its own production space (i.e. volume V) and is analogous to the fixed crystallization volume in the case of overall crystallization. This abstract (imaginary) space available for the production of items by a source (i.e. in a system) is fixed.

(2) The process of production of items is similar to a chemical reaction and involves the formation of an activated complex and its dissociation into products. This means that there are threshold free energy

changes ΔG_a and overall free energy changes $\Delta G_a + \Delta G_R$ for the generation of items. In the case of citing of published papers by authors, Vinkler [52] calls ΔG_a and ΔG_R cognitive pressure and threshold cognitive pressure, respectively.

(3) Items are produced at active centers in the available space by the formation and growth of 3D clusters or nuclei such that the time dependence of the volume $V_c(t)$ of items produced at time t occurs in the available volume $V - V_c(t)$.

(4) Items can be generated both by instantaneous and progressive nucleation (cf. Fig. B1).

(5) As in the solid nuclei composed of n growth units, nuclei of items are composed of n information units. This assumption allows the application of basic concepts and equations of 3D nucleation (see Appendix A).

(6) The fraction α of items is given as $y(t)/y_{max}$, where $y(t)$ is the cumulative number of items at time t and y_{max} is the maximum number of items.
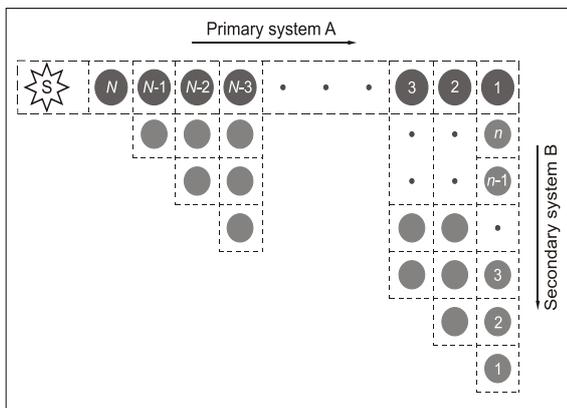

Fig. 8: Schematic illustration of processes of generation of primary items A from a source S and of secondary items B from primary items A acting as secondary sources of (secondary) items. Adapted from Sangwal [54].

In view of the above, upon replacing the fraction $\alpha = V_c(t)/V$ by $y(t)/y_{max}$, the cumulative fraction of items generated at time t from an individual source such as S in Figure 8, from Eq. (B1) of Appendix B one obtains Eq. (1), called hereafter Avrami−Weibull equation, with the time constant Θ and the exponent q given by Eqs. (B2) and (B3) for items generated by instantaneous and progressive nucleation modes. When q is given by Eq. (B3), Eq. (1) represents the progressive nucleation mechanism for the production of items [7,8.54].

It is usually observed that the cumulative fraction $\alpha(t)$ of secondary items such as citations produced by a complex system composed of successively appearing primary items (e.g. papers) from the primary source (e.g. an author) also follows a relation similar to that of Eq. (B1) with new time constant Θ and exponent q. In fact, a modeling experiment, carried out by the present author [39,53] of secondary items such as citations produced by progressive nucleation from a complex

system composed of successively appearing primary items (e.g. papers) from a primary source (e.g. author) at equal intervals of time Δ, characterized by different values of time constant Θ and exponent q, showed that Eq. (1) describes equally well the time dependence of cumulative fraction $y(t)/y_{max}$ of secondary items. However, it was observed that the values of both Θ and q increase with increasing duration t of generation of secondary sources of items.

It should be mentioned that during 1939-1941 M. Avrami proposed and popularized Eq. (1). It is known as Weibull function in the literature on microbial growth and provides a physical interpretation of its parameters. It has the form of Weibull distribution function [55]. As in a previous paper [40], in this paper Eq. (1) is referred to as Avrami−Weibull equation to honor its proponents.

From Eq. (1) one may define fraction of generated fraction of items as

$$x = \frac{y_{max} - y(t)}{y_{max}} = \exp\left\{-\left(\frac{t}{\Theta}\right)^q\right\}. \tag{13}$$

This is the so-called extended exponential used by Hirsch [18] to discuss the relationships of the maximally cited papers N_{max} and the total number $N(t_m) = 1$ of papers with at least one citation with the Hirsch index h. However, in the above function the exponent $q \leq 1$. In contrast, depending on the nucleation mode in Eq. (B1), the exponent q can take values both less than and greater than unity.

5. Predictions of Avrami−Weibull function

From analysis of data on the growth behavior of a wide range of material items, such as germination of tomato seeds, growth of bacteria in different media, and overall crystallization from melts, discussed in the preceding sections it may be concluded that Avrami−Weibull function (1) with its two parameters Θ and q explains the data much better than Verhulst (logistic) function (2) and Gompertz function (3) and the temperature dependence of its time constant Θ may be interpreted in terms of the dependence of rate constant k of chemical reactions and nucleation rate J on temperature T according to relations (A3) and (A6), respectively.

Relation (1) also explains the dependence of nucleation rate J on driving force ΔG_R involved in overall crystallization. Although the effect of temperature on the growth behavior of abstract items, such as papers and their citations, is not expected, one finds that the growth behavior of the cumulative number $y(t)$ of abstract items with time t by individual (simple) sources and collectives or groups of sources (complex sources) also follows Avrami−Weibull function (1). Moreover, as discussed in Appendix C, Avrami−Weibull function (1) is superior to Verhulst (logistic) and Gompertz functions in explaining the generation rate $dy(t)/dt$ of items in terms of the parameters Θ and q. In view of these

features, the predictions of Avrami−Weibull function are described below.

5.1. Behavior of growth curves

Figures 9a and 9b illustrate the cumulative fraction $F(t) = y(t)/y_{max}$ of items, produced by individual sources, characterized by different q at $\Theta = 20$ arbitrary units (a.u.) and by different Θ at $q = 2$, respectively, using Eq. (1). As seen from the plots of Figure 9a, irrespective of the value of Θ, curvatures of the curves are concave and convex for $q \leq 1$ and $q > 1$, respectively, but for all q the curves attain $F(t) = 1$ at sufficiently high values of Θ such that the S-shaped curves are obtained only in the latter case of $q > 1$. However, the plots show that their convex curvature increases with increasing values of Θ for a given value of $q > 1$ (Figure 9b) whereas their concave curvature increases with decreasing $q < 1$ for a given value of Θ (Figure 9a). It may be demonstrated easily that a linear dependence is obtained when $t/\Theta \ll 1$ and $q = 1$ in Eq. (1); see Appendix C.
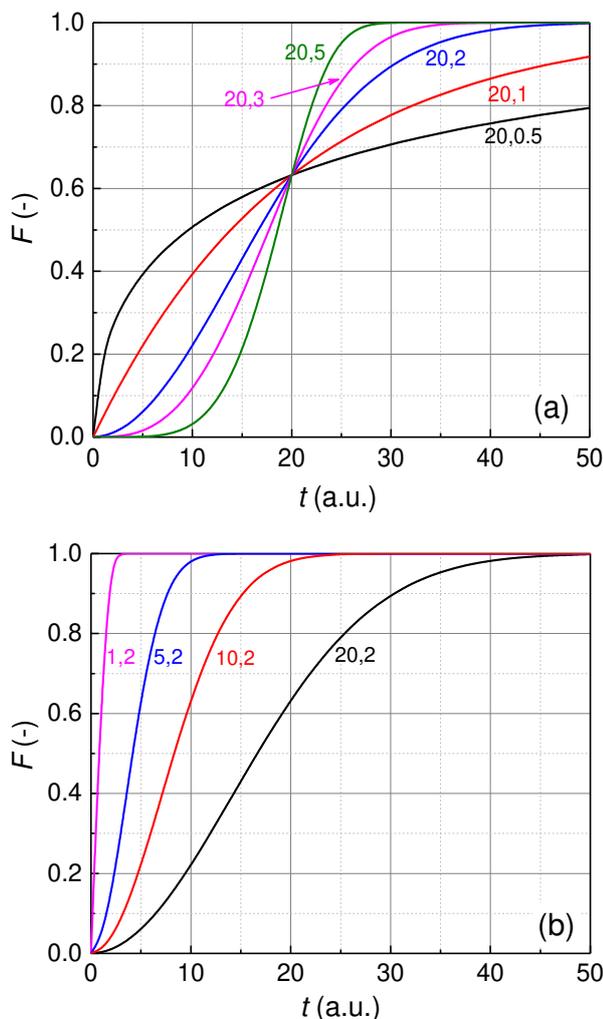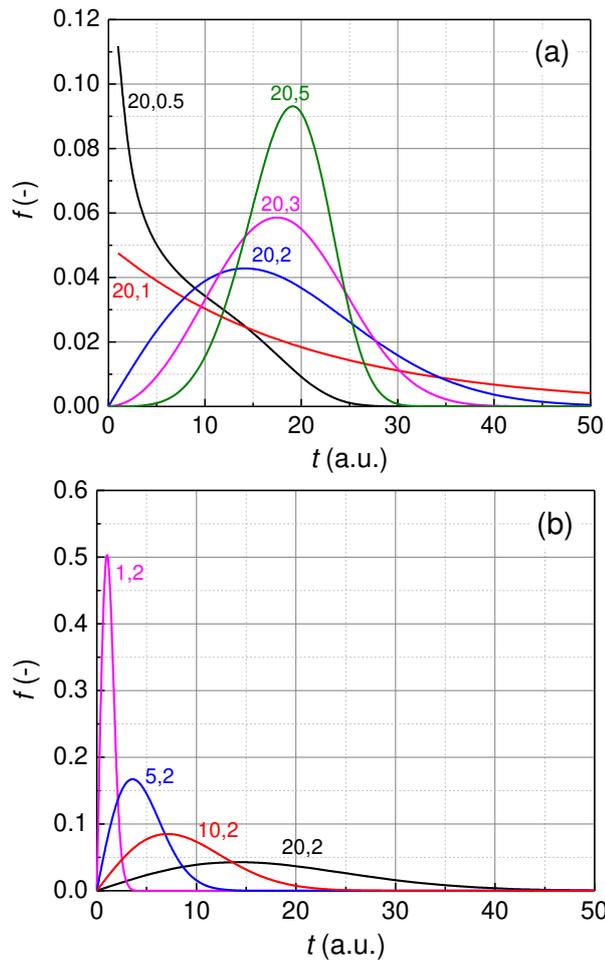

Figure 9: Cumulative fraction $F(t) = y(t)/y_{max}$ of items produced according to Avrami−Weibull function (1) by individual sources characterized by (a) different q at $\Theta = 20$ arbitrary units (a.u.) and (b) different Θ at $q = 2$. Values of Θ and q are indicated as (Θ,q) alongside the plots.

Using citation data of articles written by selected Chinese American Nobel prize winners in physics, Liu and Rousseau [56] reported three types of cumulative citation $L(t)$ plots: (1) *normal* S-shaped plots with initial convex curvature followed by concave curvature, (2) *inverse* S-shaped plots with initial concave curvature followed by convex curvature, and (3) linear plots of $L(t)$ data. Avrami−Weibull function (1) satisfactorily describes the nature of the above curves [40].

5.2. Behavior of growth rate curves

It is frequently observed that the absolute number of items per unit time (e.g. citations per year of an author; also called citation frequency and citation rate), usually defined as $\Delta L = [L(t)−L(t−1)]$ when t is taken in years Y, initially increases, then, after going through a maximum value, slowly decreases and finally attains a zero value with increasing time (for example, see: [8,39,45,57-59]). This phenomenon of slowly decreasing growth of items with time is usually called obsolescence [60-64], aging [63] or decay. In the case of citations of individual articles, typical curves of ΔL against citation time t are of the following types [62]: (a) initially much-praised articles, (b) recognized basic work, (c) scarcely reflected work, (d) well received but later erroneously qualified work, and (e) general work. According to this classification, citation rate curves with steep positive slope are characteristic of initially much-praised articles or articles that recognized basic work. This classification of growth of citation rate curves has been used recently by Ho and Kahn [59] in the discussion of top-cited single-author papers.

The above trends of citation frequency are usually explained by using empirical exponential functions [7,61,63,64]. The main criticism of using these empirical exponential functions to describe their decaying behavior is that they contain parameters to which it is difficult to assign any physical significance. However, as shown in Appendix C, the fitting parameters Θ and q of the Avrami−Weibull function have well-defined meaning.

Figures 10a and 10b show the plots of growth rate $f(t) = dF(t)/dt$ of items corresponding to the cumulative fraction $F(t) = y(t)/y_{max}$ of items of Figure 9. From these plots the following features may be noted:

(1) For a given value of the time constant Θ, with an increase in the value of the exponent q the maximum value of f_c for the items shifts to a higher t such that the value of t_c corresponding to the peak approaches the value of the time constant Θ; see Figure 10a.

(2) For a given value of the exponent q, with an increase in the value of the time constant Θ the maximum value of f_c for the generation of items shifts to a higher t such that the value of t_c corresponding to the peak is lower than the value of the corresponding time constant Θ; see Figure 10b.

(3) For a given set of Θ and q, the area under the plot of $f(t)$ for the items over the entire generation period t

represents the maximum cumulative fraction $F_{max} = 1$ of the items.

It may be seen from Figure 10 that the distribution of items generated by a source usually has a skew to the right for different sets of Θ and q. However, for a particular value of Θ, there is a value of q when the distribution is symmetrical. Conversely, for a particular value of q, there is a value of Θ when the distribution of items is symmetrical. Corresponding to $\Theta = 20$ in Figure 10a, the value of q is about 4 when the distribution of citations is symmetrical. One also expects that the distribution has a skew to the left for q exceeding about 4.

Figure 10: Plots of growth rate $f(t) = dF(t)/dt$ of items produced according to Avrami−Weibull function (1) by individual sources characterized by (a) different q at $\Theta = 20$ arbitrary units (a.u.) and (b) different Θ at $q = 2$. Values of Θ and q are indicated as (Θ,q) alongside the plots.

Figure 11 shows some typical examples of evolution of yearly citations ΔL of papers published by Laemmli and Cox with time t. In Figure 11a yearly citations of all subsequently papers published by Laemmli are compared with his top-cited paper 1 whereas in Figure 11b yearly citations to his next three top-cited papers are presented. Figure 11c shows yearly citations received by the top-cited two papers of Cox. In these figures the curves are drawn with the values of the
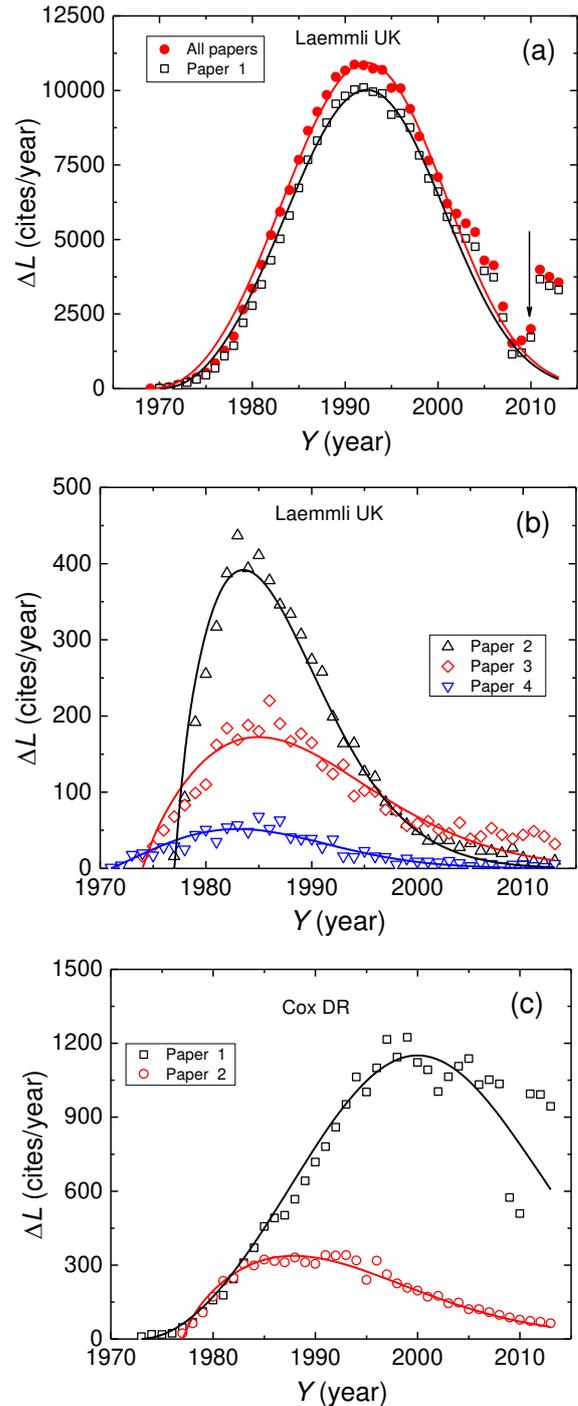

Figure 11: Typical examples of evolution of yearly citations ΔL of papers published by different authors: (a,b) Laemmli and (c) Cox. In (a) citations of all subsequently papers published by Laemmli are compared with his top-cited paper 1. Curves are drawn with best-fit parameters given in Table 4.

parameters of Eq. (1) given in Table 3. It may be seen from this table that the total yearly citations of all successively papers mainly come from the top-cited paper 1 and that the exponent q lies between 1 and 4 for all individual papers.

Analysis of growth of citations using Avrami−Weibull function to individual papers published by different authors indeed shows that $1 < q < 4$ for most cases. For example, the values of q lies between 1 and 2.7 for

citations to individual 27 top-cited papers of 4 selected Polish professors [8], between 1 and 3.2 for citations to articles by 4 of 5 Chinese American Nobel Prize winners [40], and between 0.9 and 3.5 for citations to 41 of 43 top-cited papers by 12 authors (Sangwal, unpublished results). This suggests that the process of citations received by individual articles is mainly determined by progressive nucleation mode involving both diffusion and integration of published knowledge (cf. Appendix B).

6. Summary and conclusions

Some examples of empirical data of sigmoidal-shaped $y(t)$ growth of different types of real and abstract items are analyzed by Verhulst, Gompertz and Avrami−Weibull functions. It was found that Avrami−Weibull function describes the growth behavior of different types of items better than Gompertz and Verhulst functions. Moreover, in comparison with Verhulst (logistic) and Gompertz functions, Avrami−Weibull function is relatively simple and mathematically convenient for explaining different trends of the generation rate $dy(t)/dt$ of scientific literature in terms of its two parameters: the time constant Θ and the exponent q.

Employing the basic concepts of occurrence of chemical reactions between reactants producing reaction products and overall crystallization of solid phase in melts and solutions (Appendices A and B), Avrami−Weibull function (1) for the growth behavior of cumulative number $y(t)$ items produced at time t by individual (simple) sources and collectives or groups of sources (complex sources) is presented. Then the data of germination of tomato seeds, growth of various bacteria in different media and evolution of overall crystallization of polypropylene are analyzed from the standpoint of occurrence of chemical reactions and crystallization from melts and solutions.

It is observed that every plot of the growth of cumulative number $y(t)$ of items against time t is characterized by three parameters: dimensionless growth rate $R = dy/y_{max}dt$ determined from the linear part of a $y(t)/y_{max}$ plot, time lag t_0 corresponding to the onset of initial growth, and time constant Θ when the rate R reaches a maximum value. In the case of growth of material items such as bacteria, the growth rate R increases whereas the time lag t_0 and the time constant Θ decrease with increasing temperature T. However, an opposite trend is observed in overall crystallization from the melt. In this case, the crystallization rate R decreases but the time lag t_0 and the time constant Θ increase with crystallization temperature T. The former processes are associated with chemical reactions which follow simple Arrhenius-type relation (A3) in which the cumulative volume (concentration) of reaction products decreases with an increase in ΔG_R, whereas overall crystallization follows relation (A8) in which the cumulative volume of crystallized phase increases with an increase in ΔG_R. In the latter case, the parameters R, t_0 and Θ are related to the de-

pendence of the number N_m of nuclei formed or the nucleation rate J on driving force ΔG_R.

There exists a cognitive citation pressure ΔG_R as the driving force for the citation received by a paper [51,52]. The mechanisms and processes of motivations for citation have been discussed in the scientometric research [69-71]. The cognitive citation pressure ΔG_R is essentially associated with the attractiveness of a paper to be cited. The higher the attractiveness of a paper, the higher is its citability. Comparison of the process of receiving of citations by papers with the processes of occurrence of chemical reactions and crystallization of solid phases from melts and supersaturated solutions in terms of this driving force ΔG_R shows that the process of citations of papers is similar to that of overall crystallization of solid phases. The process of overall crystallization involves the formation of nuclei of crystallized phase instantaneously or progressively with time in a fixed volume. Using an analogy with overall crystallization, it is argued that similar processes occur during the citation of papers. However, citation process differs from overall crystallization. Overall crystallization of solid phase depends on crystallization temperature but no effect of temperature can be conceived in citation process.

Analysis of growth of citations using Avrami−Weibull function to individual papers published by different authors shows that $1 < q < 4$ for most cases. This suggests that the process of citations received by individual articles is mainly determined by progressive nucleation mode involving both diffusion and integration of published knowledge.

Finally, it should be emphasized that, despite arguments in favor of similarity of citations of papers and other information production processes with overall crystallization presented here for their explanation by Avrami−Weibull function, all workers in the field of informetrics may not be convinced. However, the relatively simple and mathematically convenient form of this function does deserve due attention to describe the dynamics of growth of citations of papers and other similar processes.

Appendix A. Occurrence of chemical reactions and crystallization

The driving force for the occurrence of any chemical reaction is the difference ΔG_R in the Gibbs free energy G_I of initial reactants, say A and B, and the free energy G_{II} of the products, say C and D, and may be expressed by the relation

$$A + B \rightarrow X^* \rightarrow C + D + \Delta G_R, \qquad (A1)$$

where X^* is a transient, activated complex of free energy G^* higher than G_I of the reactants (see Figure A1). The rate of formation of products is determined by the values of these three free energies. The formation of products is possible when the free energy change $\Delta G_R > 0$, which is the necessary driving forces for the reaction, but the rate of the reaction is determined by the relative

increase in the free energy ΔG_a ($\Delta G_a = G^* - G_I$) involved in the formation of the activated complex X^*. The higher the free energy change ΔG_a required for the formation of the activated complex, the more difficult it is for the reaction to occur. Similarly, the greater the value of ΔG_R, the higher is the stability of the reaction products.
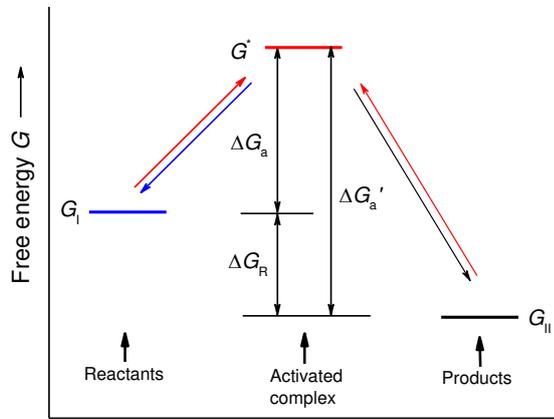

Figure A1: Schematic presentation of free energy changes associated with a chemical reaction.

The rate of the reaction (A1) may be given by (see ref. [47]; Chap. 14)

$$\text{rate} = \frac{dC_{Pr}}{dt} = k C_A C_B , \qquad (A2)$$

where C_A, C_B and C_{Pr} are concentrations of A, B and products, and k is the rate constant. According to the transition state theory of reaction rates, the rate constant

$$k = \frac{\text{rate}}{C_A C_B} = A \exp\left(-\frac{\Delta G_R^0}{R_G T}\right), \qquad (A3)$$

where ΔG_R^0 is the difference between energy of reactants and complex, all in their respective ground states, the pre-exponential factor A is frequently called the frequency factor, R_G is the gas constant, and T is the temperature in Kelvin.

According to Eq. (A3) the rate constant k for a chemical reaction involving a constant energy change ΔG_R^0 increases with temperature T. Eq. (A3) is similar in form to the Arrhenius equation relating the temperature dependence of rate constant k with activation energy ΔG_R^0 for a chemical reaction. An Arrhenius-type equation also holds for diffusion and fluidity processes in solutions [65].

As in the case of chemical reactions, crystallization from melts and solutions is also associated with two energy changes: an activation barrier ΔG_{3D}^* for the formation of three-dimensional (3D) clusters or nuclei in the liquid phase, given by Eq. (A7), and an overall change in the free energy ΔG_R, given by Eq. (A1). The value of the activation barrier ΔG_{3D}^* is associated with the formation of 3D clusters by aggregation of growth entities (e.g. atoms, ions and molecules) present in the liquid, whereas the overall change in the free energy

ΔG_R determines whether the 3D clusters formed in the growth system remain stable after their formation. Note that the free energy change ΔG_R is a measure of deviation from equilibrium state when $\Delta G_R = 0$, and $\Delta G_R > 0$ for supersaturated solutions. While discussing the process of formation of clusters it is usually assumed that they prefer to attain a rounded shape of radius r because the surface tension γ of a sphere is the lowest. However, in view of analysis of the number of items in this paper we discuss the process of formation of these clusters in the medium in terms of free energy change as a function of the number n of atoms, ions or molecules comprising them.
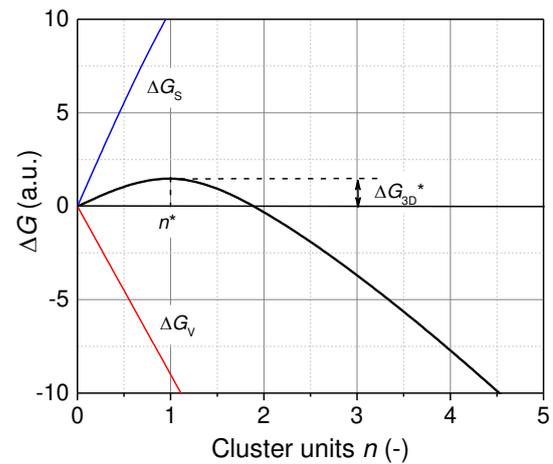

Figure A2: Change in Gibbs free energy ΔG as a function of size n of clusters forming in a supersaturated medium. Values for surface energy $\gamma = 11.25$ and driving force $\Delta G_R = 9$ are chosen to obtain critical nucleus with $n = 1$. ΔG_R and γ are expressed in the same arbitrary energy units (a.u.). Curves of energy contributions ΔG_S and ΔG_V are also shown.

The reduction in the Gibbs free energy ΔG of a system due to the formation of a 3D cluster composed of n growth units is equal to the sum of the surface excess free energy ΔG_S and the volume excess free energy ΔG_V. The resulting free energy change may be given by [66,67]

$$\Delta G = \Delta G_S + \Delta G_V = n^{2/3}\gamma - n\Delta G_R , \qquad (A4)$$

where γ is a surface-energy term. The two terms in the right-hand side of Eq. (A4) depend differently on n. This behavior of ΔG associated with the formation of the cluster is shown in Figure A2 as a function of its size n. It may be seen from the figure that ΔG passes through a maximum and the maximum value ΔG_{3D}^* corresponds to the critical size n^*. The value of n^* may be obtained by maximizing Eq. (A4), taking $d\Delta G/dn = 0$, i.e.

$$\frac{d\Delta G}{dr} = \frac{2}{3}n^{-1/3}\gamma - \Delta G_R = 0 , \qquad (A5)$$

or

$$n^* = \left(\frac{2}{3}\frac{\gamma}{\Delta G_R}\right)^3 . \qquad (A6)$$

Upon substituting the value of n^* from Eq. (A6) into Eq. (A4), one obtains the energy barrier

$$\Delta G_{3D}^* = \frac{4}{27}\frac{\gamma^3}{(\Delta G_R)^2} = \frac{1}{3}n^{*2/3}\gamma . \qquad (A7)$$

Note that the value of ΔG_{3D}^* is always a positive quantity. Obviously, increasing free energy difference ΔG_R and decreasing interfacial energy γ facilitate the formation of 3D clusters.

Occurrence of a crystalline phase in a supersaturated medium depends on the size n of the nuclei. When $n < n^*$, the nuclei dissolve. However, when $n > n^*$, the nuclei are stable and grow. The critical size n^* is the minimum size of a stable nucleus. As seen from Figure A2, only when the nucleus size $n > n^*$, the free energy ΔG for the formation of a nucleus decreases with an increase in its size n.

At constant temperature and supersaturation conditions, the occurrence of 3D cluster formation (or nucleation) is described by the so-called stationary nucleation rate J, given by [66]

$$J = J_0 \exp\left(-\frac{\Delta G_{3D}^*}{R_G T}\right) = J_0 \exp\left(-\frac{B}{(\Delta G_R)^2}\right), \qquad (A8)$$

where J_0 is a kinetic factor and is associated with the frequency of attachment of basic units to the nucleus at equilibrium, ΔG_{3D}^* is given by Eq. (A7) and $B = 4\gamma^3/27R_G T$.

Eq. (A8) represents the temperature dependence of nucleation rate J, and is usually referred to as the classical theory of 3D nucleation. Obviously, it is an Arrhenius-type relation where the activation barrier ΔG_{3D}^* is essentially a measure of the "difficulty" for atomic/molecular aggregates to attain the size n^* of the stable clusters in a growth medium.

It should be mentioned that the free energy difference ΔG_R is not a temperature independent quantity, and is given by (for example, see: [36,67])

$$\Delta G_R = \left(\frac{\Delta H_m}{T_m}\right)(T_m - T) , \qquad (A9)$$

where ΔH_m is the enthalpy of melting of the compound, T_m is the its melting point, and T is the crystallization temperature. Obviously, crystallization from the melt is possible when the temperature difference $\Delta T = (T_m - T) > 0$. Then the nucleation rate (for example, see: [36,67])

$$J = J_0 \exp\left(-\frac{B'}{T(\Delta T)^2}\right), \qquad (A10)$$

with the constant

$$B' = \frac{\kappa}{\phi^2}\left(\frac{\gamma}{R_G}\right)^3 , \qquad (A11)$$

where κ is the geometrical factor for the shape of clusters (here $\kappa = 4/27$), and the parameter $\phi = \Delta H_m / R_G T_m$ is about 2 for metals, 3 for anhydrous inorganic salts, and 6 for organic compounds.

Eq. (A10) differs fundamentally from Arrhenius-type relation (A3) in the T-term. Under crystallization conditions, in Eq. (A10) the crystallization temperature $T \approx T_m$ but the temperature difference $\Delta T = (T_m - T)$ rapidly increases with small increases in T. Therefore, the nucleation rate J essentially depends on ΔT instead of T, with an activation energy B' in the plots of $\ln J$ against $T(\Delta T)^2$.

Appendix B: Basic concepts of overall crystallization

Description of overall crystallization of a solid phase in the volume of a melt or supersaturated solution is one of the various applications of the theory of nucleation in the field of crystal growth. The theory of overall crystallization is based on the following concepts [66]:

(1) The fraction α of solid phase is the total volume $V_c(t)$ of solid phase crystallized after time t in the initial fixed volume V of the crystallizing system: $\alpha = V_c(t)/V$.

(2) The volume $V_c(t)$ of the solid phase is formed by its nucleation at material points at a rate $J(t)$ in the volume V of the crystallizing medium (melt or supersaturated solution) and each nucleus grows independently of the other nucleating and growing crystallites. This means that crystallites can be nucleated only in the noncrystallized volume $V - V_c$ of the crystallizing medium.

(3) Nuclei can form on active centers in the medium either instantaneously at $t = 0$ or progressively during the entire crystallization process, thereby determining the time dependence of nucleation on active centers and finally the overall crystallization of the solid phase resulting from the growth of the nuclei in the liquid phase. These types of growth are known to occur by instantaneous and progressive nucleation modes, respectively, and are illustrated in Figure B1.

With the above ideas of the fraction $\alpha(t)$ of solid phase crystallized at time t, the total volume $V_c(t)$ of the solid phase crystallized after time t in the initial fixed volume V of the crystallizing system by instantaneous and progressive nucleations may be given by the unified relation [66]

$$\alpha(t) = \frac{V_c(t)}{V} = 1 - \exp\left\{-\left(\frac{t}{\Theta}\right)^q\right\}, \qquad (B1)$$

where Θ is a time constant, and the exponent $q > 0$. The exponent q and the time constant Θ are given by
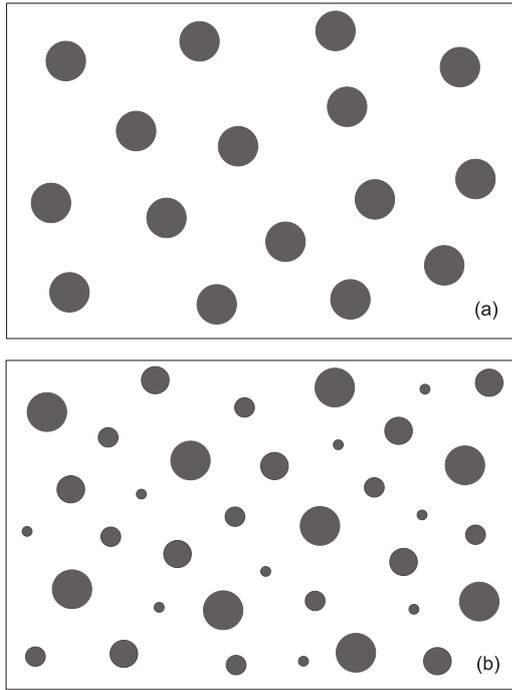
Figure B1: Schematic illustration of (a) instantaneous and (b) progressive formation of nuclei of a solid phase at active centers in a fixed volume of melt or supersaturated solution.

$$q = vd, \quad \Theta = \frac{1}{g}\left(\frac{V}{\kappa N_{\mathrm{m}}}\right)^{1/vd}, \tag{B2}$$

for instantaneous nucleation, and

$$q = 1 + vd, \quad \Theta = \left(\frac{1+vd}{\kappa g^{vd} J_{\mathrm{s}}}\right)^{1/(1+vd)} \tag{B3}$$

for progressive nucleation. In Eqs. (B2) and (B3) N_{m} is the maximum number of nucleation centers, J is the rate of stationary nucleation given by Eq. (A8), κ is the shape factor for the nuclei (for example, $\kappa = 4\pi/3$ for spherical nuclei) and the growth constant g is defined by

$$g = \frac{r^{1/v}}{t}, \tag{B4}$$

where r is the radius of the growing nucleus and the constant $v > 0$ is a number. Eq. (B4) describes the dependence of the radius r of the growth of *individual* nuclei on time t according to the traditional power-law relation

$$r(t) = Zt^{v}, \tag{B5}$$

where the values of v are 1/2 and 1 for growth controlled by volume diffusion and interface transfer, respectively, and $Z = g^{v}$. In Eqs. (B2) and (B3) the parameter d denotes the dimensionality of growing nuclei. For nuclei growing in one-, two- and three-dimensions, $d = 1, 2$ and 3, respectively. However, when the nuclei do not grow, $d = 0$.

Aggregation of growth entities into nuclei and their subsequent growth into stable entities involves diffusion of growth entities to active nucleation centers present in the melt or solution volume and integration of these growth units into the surface of the nuclei. Therefore, the value of the exponent q in Eqs. (A2) and (A3) depends on the values of the exponent v, the dimensionality d and the nucleation mode. In the case of instantaneous nucleation mode, $0 < q < 1.5$ and $0 < q < 3$ for crystallization controlled by volume diffusion and interface integration, respectively. However, when crystallization occurs by progressive nucleation mode, $1 < q < 2.5$ and $1 < q < 4$ for crystallization controlled by volume diffusion and interface integration, respectively. The lowest values of 0 and 1 for q, corresponding to crystallization by instantaneous and progressive nucleation mechanisms, respectively, are obtained when the nuclei do not grow with t.

Note that the exponent q is a non-integer parameter in diffusion-controlled crystallization but it is usually found that it also has non-integer values even in mass-transfer-controlled crystallization due to different assumptions used in the derivation of Eq. (B1). The time constant Θ is determined by the growth constant g and either by the maximum number N_{m} of crystallites in instantaneous nucleation mechanism (Eq. (B2)) or by stationary nucleation rate J_{s} in progressive nucleation mechanism (Eq. (B3)).

The above treatment is usually called the Kolmogorov−Johnson−Mehl−Avrami (KJMA) theory. However, in the literature on crystallization of fats it is also known as the Avrami equation in which mass instead of volume is used and the exponential term $(t/\Theta)^{q} = kt^{q}$, where k is the Avrami constant and q is the Avrami exponent [68]. Theoretical aspects of this theory for overall crystallization are discussed by Kashchiev [66].

It should be mentioned that real kinetic rate laws are not as simple as described by Eq. (A2) where the rate of formation of reaction product is directly related to the concentrations C_{A} and C_{B} of reactants A and B. For example, there are consecutive reactions in which intermediates interact with the reactants and the products and in which various types of elementary reactions and their combinations take place [49]. In this sense, the Avrami constant k is a complex constant of qth order.

Appendix C. Comparison of predictions of different functions

All of the above three functions relating cumulative distribution function $F(t) = y(t)/y_{\mathrm{max}}$ with t, described in Section 2, are two-parameter functions but they predict different trends of the plots of $y(t)$ and $dy(t)/dt$ against time t. Avrami−Weibull and Gompertz functions predict $y(t) = 0$ at $t = 0$ but according to Verhulst function $y(t) = y_0 > 0$ at $t = 0$. This means that Verhulst function is not expected to explain satisfactorily situations of empirical data with $y(t) = 0$ at $t = 0$. However, the three functions predict an initial increase in $dy(t)/dt$, followed by a subsequent decrease, with t such that $dy(t)/dt$ attains a max-

imum value $[dy(t)/dt]_c$ at a particular value of t, say t_c. The trends of the dependence of $dy(t)/dt$ on t predicted by the three functions are different. The value of t_c when $dy(t)/dt$ attains its maximum value may be obtained by maximizing Eqs. (1), (2) and (3).

In the case of Avrami–Weibull relation (1) the rate R of generation $y(t)$ of items with t may be given by

$$R = \frac{dy(t)}{dt} = y_{\max} \frac{q}{\Theta^q} t^{q-1} \exp\left\{-\left(\frac{t}{\Theta}\right)^q\right\}. \tag{C1}$$

Eq. (C1) predicts an initial increase in the generation rate R of items according to power law and, after reaching a maximum value at time t_c, it decreases exponentially. From Eq. (C1) one has

$$\frac{dR}{dt} = \frac{d^2 y(t)}{dt^2} = y_{\max} \frac{q}{\Theta^q} t^{q-1} \exp\left\{-\left(\frac{t}{\Theta}\right)^q\right\}\left[\frac{q-1}{t} - \frac{q}{\Theta^q}\right]$$

$$= \frac{dy(t)}{dt}\left[\frac{q-1}{t} - \frac{q}{\Theta^q} t^{q-1}\right] = 0, \tag{C2}$$

which gives

$$t_c = \left(\frac{q-1}{q}\right)^{\frac{1}{q}} \Theta. \tag{C3}$$

Substitution of t_c from Eq. (C3) into Eq. (C2) gives the maximum rate $R_c = (dy(t)/dt)_c$ in the form

$$R_c = \left(\frac{dy(t)}{dt}\right)_c = y_{\max} \frac{q}{\Theta}\left(\frac{q-1}{q}\right)^{\frac{q-1}{q}} \exp\left[-\left(\frac{q-1}{q}\right)\right]. \tag{C4}$$

According to the above equations t_c and R_c depend on the parameters q and Θ. Note that a maximum rate R_c is not achieved when $0 < q < 1$ (see Figure 10). Then $t_c = 0$ and $(dy(t)/dt)_c = 0$ (see Eqs. (C3) and (C4)).

According to Verhulst function (2) the items' generation rate R with time t is given by

$$R = \frac{dy(t)}{dt} = \beta y(t)\left(1 - \frac{y(t)}{y_{\max}}\right). \tag{C5}$$

From (C5) one obtains

$$\frac{dR}{dt} = \frac{d^2 y(t)}{dt^2} = \beta\left(1 - 2\frac{y(t)}{y_{\max}}\right) = 0, \tag{C6}$$

which gives

$$y(t_c) = \frac{y_{\max}}{2}. \tag{C7}$$

Substitution of $y(t_c)$ from Eq. (C7) into Eq. (C5) gives the maximum R_c in the form

$$R_c = \left(\frac{dy(t)}{dt}\right)_c = \frac{\beta y_{\max}}{4}. \tag{C8}$$

Obviously, R_c depends only on the value of the parameter β and is independent of y_0 and time t.

In the case of Gompertz function (3) the items' generation rate

$$R = \frac{dy(t)}{dt} = y_{\max}\lambda(\exp ct)\exp\left\{-\frac{\lambda}{c}(\exp ct - 1)\right\}. \tag{C9}$$

Eq. (C9) predicts both increase and decay in $y(t)$ with time t following exponential dependences, exhibiting maximum R_c at t_c. From (C9) one has

$$\frac{dR}{dt} = \frac{d^2 y(t)}{dt^2} = y_{\max}\lambda^2 \exp(2ct)\exp\left\{-\frac{\lambda}{c}(\exp ct - 1)\right\} = 0, \tag{C10}$$

which gives

$$t_c = \frac{1}{c}\ln\left(1 - \frac{c}{\lambda}\right). \tag{C11}$$

Substitution of t_c from Eq. (C11) into Eq. (C9) gives the maximum R_c in the form

$$R_c = y_{\max}\lambda \exp\left(1 - \frac{c}{\lambda}\right). \tag{C12}$$

According to the above equations t_c and R_c depend on the parameters c and λ. Note that a maximum value of R is not achieved when $c \ll \lambda$. Then $t_c = 0$ and $R_c = 2.718 y_{\max}\lambda$ (cf. Eqs. (C11) and (C12)).

According to power-law relation (3), the items generation rate R may be given by

$$R = \frac{dy(t)}{dt} = y_{\max} \frac{q}{\Theta^q} t^{q-1}. \tag{C13}$$

Obviously, the rate R is also expected to follow power-law dependence. Similarly, for $ct \ll 1$, Gompertz function (3) gives

$$R = y_{\max}\lambda \exp\{(c - \lambda)t\}. \tag{C14}$$

Depending on the value of $c > \lambda$, Eq. (C14) predicts an exponential increase in R with t. For $q = 1$ and $c = \lambda$, (C13) and (C14) reduce to the form

$$R = y_{\max}\lambda, \tag{C15}$$

with $\lambda = 1/\Theta$.

In summary, although Verhulst and Gompertz functions (2) and (3) predict the appearance of maximum rate R_c, their parameters β, and c and λ do not give any insight into the processes involved in the growth of items. In contrast to them, Avrami–Weibull relation (1) not only explains the growth of items with time t better than the Verhulst and Gompertz functions as well as maximum values of R_c through its parameters Θ and q but these parameters have physical meaning.

Acknowledgements

References

[1] D.D.S. Price, Little Science, Big Science. Columbia University Press, New York & London, 1963.

[2] L. Egghe, I.K. Ravichandra Rao, Classification of growth models based on growth rates and its applications, Scientometrics 25 (1992) 5-46.

[3] B.M., Gupta, L. Sharma, C.R. Karisiddappa, Modeling the growth of papers in a scientific speciality, Scientometrics 33(2), (1995) 187-201.

[4] B.M., Gupta, S. Kumar, S.L. Sangam, C.R. Karisiddappa, Modeling the growth of social science literature, Scientometrics 53(1), (2002) 161-164.

[5] I.K. Ravichandra Rao, D. Srivastava, Growth of journals, articles and authors in malaria research, Journal of Informetrics 4(1), (2010) 249-256.

[6] C.-Y. Wong, K.-L. Goh, Growth behavior of publications and patents: A comparative study on selected Asian economies, Journal of Informetrics 4(2), (2010) 460-474.

[7] K. Sangwal, Progressive nucleation mechanism and its application to the growth of journals, articles and authors in scientific fields, Journal of Informetrics 5(4), (2011) 529-536.

[8] K. Sangwal, Application of progressive nucleation mechanism for the citation behavior of individual papers of different authors,. Scientometrics 92(2), (2012) 643-655.

[9] Q.L. Burrell, The nth-citation distribution and obsolescence, Scientometrics 53(3), (2002) 309-323.

[10] Q.L. Burrell, Hirsch's h-index: A stochastic model, Journal of Informetrics 1(1), (2007) 16-25.

[11] Q.L. Burrell, On the h-index, the size of the Hirsch core and Jin's A-index, Journal of Informetrics 1(2), (2007) 170-177.

[12] Q.L. Burrell, The individual author's publication–citation process: theory and practice, Scientometrics 98(1), (2014) 725-742.

[13] W. Glänzel, On the possibility and reliability of predictions based on stochastic citation processes, Scientometrics 40(3), (1997) 481-492.

[14] W. Glänzel, A. Schubert, Predictive aspects of a stochastic model for citation processes, Information Processing and Management 31(1), (1995) 69-80.

[15] X. Zheng, Predicting publication productivity for researchers: A piecewise Poisson model, Journal of Informetrics 14(3), (2020) 101065.

[16] S.Nadarajan, S. Kotz, Models for citation behavior, Scientometrics 72(2), (2007) 291-305.

[17] M.V. Simkin, V.P. Roychowdhury, A mathematical theory of citing, Journal of American Society for Information Science and Technology 58(11), (2007) 1661-1673.

[18] J.E. Hirsch, An index to quantify an individual's scientific research output, Proceedings of the National Academy of Sciences of the USA 102(46), (2005), 16569-16572.

[19] A. Fernandez, C. Salmeron, P.S. Fernandez, A. Martinez, Application of a frequency distribution model to describe the thermal inactivation of two strains of Becillus cereus,

Trends in Food Science and Technology 10(4-5), (1999) 158-162.

[20] J.-C. Augustin, A. Brouillaud-Delattre, L. Rosso, V. Carlier, Significance of Inoculum size in the lag time of Listeria monocytogenes, Applied and Environmental Microbiology 66(4), (2000) 1706-1710.

[21] M. Valero, S. Leontidis, P.S. Fernandez, A. Martinez, M.C. Salmeron, Growth of Bacillus cereus in natural and acidified carrot substrates over the temperature range 5-30°C, Food Microbiology 17(6), (2000) 605-612.

[22] H. Fujizawa, A. Kai, S. Morozumi, A new logistic model for bacterial growth, Journal of the Food Hygienic Society of Japan 44(3), (2003) 155-160.

[23] H. Fujizawa, A. Kai, S. Morozumi, A new logistic model for Escherichia coli growth at constant and dynamic temperatures. Food Microbiology 21(5), (2004) 501-509.

[24] M.G. Corradini, M. Peleg, A Weibullian model for microbial injury and mortality, International Journal of Food Microbiology 119(3), (2007) 319-328.

[25] M. Peleg, M.G. Corradini, M.D. Normand, The logistic (Verhulst) model for sigmoidal microbial growth curves revisited, Food Research International, 40(7), (2007) 808-818.

[26] G.T., Yates, T. Smotzer, On the phase lag and initial decline of microbial growth curves, Journal of Theoretical Biology 244(3), (2007) 511-517.

[27] G.M.F., Aragao, M.G., Corradini, M.D., Nonmand, M. Peleg, Evaluation of the Weibull and log normal distribution functions as survival models of Escherichia coli under isothermal and non-isothermal conditions, International Journal of Food Microbiology 119(3), (2007) 243-257.

[28] M.Y. Li, X.M. Sun, G.M. Zhao, X.Q. Huang, J.W. Zhang, W. Tian, Q.H. Zhang, Comparison of mathematical models of lactic acid bacteria growth in vacuum-packaged raw beef stored at different temperatures, Journal of Food Science 78(4), (2012) M600-M604.

[29] J. Kowalik, A. Lobacz, Development of a predictive model for describing the growth of Yersinia enterocolitica in Camembert-type cheese, International Journal of Food Science and Technology 50(3), (2015) 811-818.

[30] A. Lobacz, J. Kowalik, A predictive model for Listeria monocytogenes in UHT diary products with various fat content during storage, Journal of Food Safety 35(1), (2015) 119-277.

[31] S. Sakanoue, Extended logistic model for growth of single-species population, Ecological Modelling 205(1-2), (2007) 159-168.

[32] H. Krug, G. Taubert, Practical use of the logistic law in experimental tumor-growth, Archiv für Geschwulstforsch 55(4), (1985) 235-244.

[33] U. Foryś, A. Marciniak-Czochra, Logistic equations in tumour growth modelling, International Journal of Applied Mathematical Computation Science 13(3), (2003) 317-325.

[34] B. Gładyszewska, Ocena wpływu przedsiewnej laserowej biostymulacji nasion pomidorów na proces ich kiełkowania (Evaluation of presowing laser biostymulation of tomato seeds on the process of their germination), PhD thesis, Agriculture Academy, Lublin (1998).

[35] W. Kloek, P. Walstra, T. van Vliet. Crystallization kinetics of fully hydrogenated palm oil in sunflower oil mixtures, Journal of American Oil Chemistry Society 77(4), (2000) 389-398.

[36] S. Padar, S.A.K. Jeelani, E.J. Windhab, Crystallization kinetics of cocoa fat systems: Experiments and modeling,

Journal of American Oil Chemists' Society 85(12), (2009) 1115-1126.

[37] K. Sangwal, K. Sato, Nucleation and crystallization kinetics of fats. In: A.G. Marangoni (Editor), Structure-function analysis of edible fats, AOCS Press, Urbana, 2012, Chapter 2, pp. 25-78.

[38] L.M. Cunha, F.A.R. Oliveira, J.C. Oliveira, Optimal experimental design for estimating the kinetic parameters of processes described by the Weibull probability distribution function, Journal of Food Engineering 37(1), (1998) 175-191.

[39] K. Sangwal, Growth dynamics of citations of cumulative papers of individual authors according to progressive nucleation mechanism: concept of citation acceleration, Information Processing and Management 49(4), (2013) 757-772.

[40] K. Sangwal, On the growth dynamics of citations of articles by some Nobel Prize winners, Journal of Informetrics 9 (2015) 466-476.

[41] M.F. Brilhante, M.I. Gomes, D. Pestana, Extensions of Verhulst model in population dynamics and extremes. Chaotic Modeling and Simulation (CMSIM), Issue 4, (2012) 575-591.

[42] T. Chatterjee, B.K. Chatterjee, D. Majumdar, P. Chakrabarti, Antibacterial effect of silver nanoparticles and the modeling of bacterial growth kinetics using a modified Gompertz model, Biochimica et Biophysica Acta 185(2), (2015) 299-306.

[43] A. El-Gohary, A. Alshamrani, A.N. Al-Otaibi, The generalized Gompertz distribution, Applied Mathematical Modelling 37(1), (2013) 13-24.

[44] A.A. Jafari, A. Tahmasebi, M. Alizadeh, The beta-Gompertz distribution, Revista Colombiana de Estadistica, 37(1), (2014) 139-156.

[45] K.Y. Chuang, Y.S. Ho, Bibliometric profile of top-cited single-author articles in the Science Citation Index Expanded, Journal of Informetrics 8 (2014) 951-962.

[46] G. Leubner-Metzger, Functions and regulation of β-1,3-glucanases during seed germination, dormancy release and after-ripening, Seed Science Research 13(1), (2003) 17–34.

[47] K. Weitbrecht, K, Müller, G. Leubner-Metzger, First off the mark: Early seed germination, Journal of Experimental Botany 62(10), (2011) 3289–3309.

[48] M.A. Lopez-Manchado, J. Biagiotti, L. Torre, J.M. Kenny, Effects of reinforcing fibers on the crystallzation of polypropylene, Polymer Engineering Science 40(10), (2000) 2194-2204.

[49] D.F. Eggers, N.W. Gregory, G.D. Halsey, B.S. Rabinovitch, Physical Chemistry. Wiley, New York, 1964.

[50] J.W. Atkinson, An Introduction to Motivation. Van Nostrand, Princeton, 1964.

[51] P. Vinkler, A quasi-quantitative citation model, Scientometrics 12 (1987) 47–72.

[52] P. Vinkler, Comparative investigation of frequency and strength of motives towards referencing: The reference threshold model, Scientometrics 43(1) (1998) 107-127.

[53] K. Sangwal, Progressive nucleation mechanism for the growth behavior of items and its application to cumulative papers and citations of individual authors, Scientometrics 92(2), (2012) 575-591.

[54] K. Sangwal, Czochralski method of crystal growth in the scientific literature: An informetric study, Acta Physica Polonica B 124(2), (2013) 173-180.

[55] W. Weibull, A statistical distribution function of wide applicability, Journal of Applied Mechanics 18(3), (1951) 293–297.

[56] Y.X. Liu, R. Rousseau, Citation analysis and the development of science: A case study using articles by some Nobel Prize winners, Journal of American Society for Information Science and Technogy 65(2), (2014) 281-289.

[57] K. Sangwal, On the growth of citations of publication output of individual authors, Journal of Informetrics 5(4), (2011) 554-564.

[58] K. Sangwal, On the growth behavior of yearly citations of cumulative papers of individual authors, Journal of Scientometric Research 2(1), (2013) 30-36.

[59] Y.-S. Ho, M. Kahn, A bibliometric study of highly cited reviews in the Science Citation Index Expanded^{TM}, Journal of American Society for Information Science and Technology 65(2), (2014) 372-385.

[60] E.S. Aversa, Citation patterns of highly cited papers and their relationship to literature aging: A study of the working literature, Scientometrics 7(3-6), (1985) 383-389.

[61] A. Avramescu, Actuality and obsolescence of scientific literature, Journal of American Society for Information Science 30(4), (1979) 296-303.

[62] L. Egghe, On the influence of growth on obsolescence, Scientometrics, 27(2), (1993) 195-214.

[63] L. Egghe, I.K. Ravichandra Rao, R. Rousseau, On the influence of production on utilization functions: Obsolescence or increased use? Scientometrics 34(2), (1995) 285-315.

[64] U. Gupta, Obsolescence of physics literature: Exponential decrease of the density of citations to Physical Review articles with age, Journal of American Society for Information Science 41(4), (1990) 282-287.

[65] A.L. Horvat, Handbook of Electrolyte Solutions: Physical Properties, Estimation and Correlation Methods. Ellis Horwood, Chichester (1985).

[66] D. Kashchiev, Nucleation: Basic Theory with Applications. Butterworth-Heinemann. Oxford, 2000.

[67] J.W. Mullin, Crystallization, 4th Edition. Butterworth-Heinemann, Oxford, 2001.

[68] A.G. Marangoni, On the use and misuse of the Avrami equation in the characterization of the kinetics of fat crystallization, Journal of American Oil Chemists' Society 75(10), (1998) 1465-1467.

[69] S. Bonzi, H.W. Snyder, Motivations for citation: A comparison of self citation and citation to others. Scientometrics 21 (1991) 245–254.

[70] M.H.C. Ho, J.S. Liu, The motivations for knowledge transfer across borders: the diffusion of data envelopment analysis (DEA) methodology, Scientometrics 94 (2013) 397–421 .

[71] D. Lyu, X. Ruan, J. Xie, Y. Cheng, The classification of citing motivations: a meta-synthesis, Scientometrics 126 (2021) 3243–3264.